1984-01-01

Heat transfer and two-phase flow during shell-side condensation

Marto, P.J.

Taylor & Francis

Journal Name: Heat Transfer Eng.; (United States); Journal Volume: 5:1/2
http://hdl.handle.net/10945/60948

Heat Transfer and Two-Phase Flow during Shell-side Condensation

P. J. MARTO

Department of Mechanical Engineering, Naval Postgraduate School, Monterey, California 93943

This paper surveys the evolution of power condenser tube bundle arrangements and examines present-day designs. Condensation heat transfer during shell-side flow is reviewed, including the effects of vapor shear, condensate inundation, noncondensable gases, and enhancement techniques. The difficulties experienced in calculating vapor pressure drop through tube bundles are described, as well as recent attempts to obtain more reliable correlations. The modeling of these phenomena to predict shell-side condenser performance is reviewed, as well as the use of one- and two-dimensional computer codes. Appropriate topics for future research are identified.

INTRODUCTION

Shell-side condensation plays an important role in a variety of engineering applications including electric power, shipboard propulsion, refrigeration, and chemical processing plants. Since 1765, when James Watt conceived the idea of using a separate surface condenser in a steam engine [1], the condenser has undergone numerous changes in size, shape, and construction [2]. Until recently, however, these changes have taken place with little interaction between condenser designers and their counterparts in engineering research. This was caused in part by a lack of comprehension of the complex processes that occur when vapor, containing some noncondensable gases, flows at high velocities into a bundle of tubes through which cold water is flowing.

Today, significant insight has been gained into the two-phase flow and heat transfer phenomena that occur on the shell side of surface condensers. As a consequence, we now have the ability to more clearly picture all the physical processes that occur within a condenser and model them mathematically. In addition, the advent of digital computers with large storage capacity has made it feasible to incorporate these models into comprehensive computer codes that can predict performance under various operating conditions. When these advances are coupled with the latest research developments in two-phase heat transfer enhancement, it is clear that we are on the threshold of an era where more compact, more efficient, and less costly condensers can be reliably built for modern applications.

This paper describes the evolution of condenser bundle designs and heat transfer technology and presents a critical review of heat transfer and two-phase flow during shell-side condensation. Current developments in computer modeling of condensers are also reviewed, as well as the potential benefits of enhancing heat transfer. New directions for promising research in these areas are provided throughout the paper. While an attempt has been

This work was funded in part by the David W. Taylor Naval Ship Research and Development Center. The author wishes to extend his sincere thanks to the Heat Transfer Fluid Flow Service, Harwell, U.K., for providing a valuable literature search on this subject.

made to make the paper as comprehensive as possible, most of the information pertains to steam surface condensers such as exist in the electric power industry and in marine propulsion plants. Topics such as binary condensation, plate fin heat exchangers, and vertical tube condensers are not treated.

DEVELOPMENTS IN CONDENSER TECHNOLOGY

It is well known that in any vapor power cycle, heat rejection in the condenser is a vital part of the cycle, and the purpose of the condenser is to reject the heat at the lowest possible vapor temperature (and therefore pressure) so that a high thermodynamic efficiency is achieved [3]. A secondary purpose of the condenser is to recover the feedwater for return to the boiler [1, 4]. It is also well known that the lowest pressure in a vapor power cycle occurs within the condenser so that all the noncondensable gases that either leak into the plant or are generated due to feedwater treatment collect there and must be removed. Silver [5], in a comprehensive review of the theory of surface condensers, points out that, in addition to the above, a condenser should produce condensate with a small amount of subcooling to minimize the need to reheat it to the saturation temperature in the boiler and to minimize absorption of air and other noncondensables. These gases must be removed from the condenser, and care should also be taken to ensure that the amount of steam withdrawn with them is as small as possible, minimizing the need for feedwater makeup into the boiler. These last two conditions require that the condensate be reheated close to saturation conditions by integral contact with fresh steam and that the gases be cooled just prior to their removal. All of the above, of course, should be accomplished with a minimum vapor pressure drop. In surveying the history of surface condenser designs, it is clear that much of the evolution of bundle geometries has occurred in order to accomplish these last conditions.

Evolution of Bundle Designs

An excellent review of the early history of surface condensers was provided by Silver [1] and Sebald [2]. Although Watt introduced the concept of the surface condenser in 1765, it is apparent that practical problems with soldered joints precluded its real use until the middle of the 19th century, when the requirement for surface condensers was established with the advent of high-pressure boilers in marine power plants. Throughout the latter part of the 19th century, these devices were designed and built with considerable practical experience but with little theoretical knowledge. Figure 1 shows an early bundle layout from a patent by George Weir and James Weir in 1879 [1]. Their design required that the steam be forced to pass upward through a tightly spaced bundle of tubes so that it was in integral contact with the condensate falling to the bottom. In this way, condensate subcooling was minimized. Their design also stated that the air extraction point should be as far away as possible from the steam inlet, and for this reason baffles were placed in the top of the condenser to elongate the steam flow path.

The advent of the steam turbine at the turn of the century required that steam entry be from the top of the condenser rather than the bottom. This change in steam direction required several modifications to condenser bundle designs. The condenser shell was made circular and the steam entered from the top into a full, tightly packed bundle of tubes with an air cooler section at the bottom. This design, however, led to a large vapor pressure drop and a sizable condensate subcooling. Designs during the next 20–30 yr attempted to eliminate these deficiencies [2]. Figure 2 shows four variations in circular condenser bundle geometry. In Fig. 2*a*, the

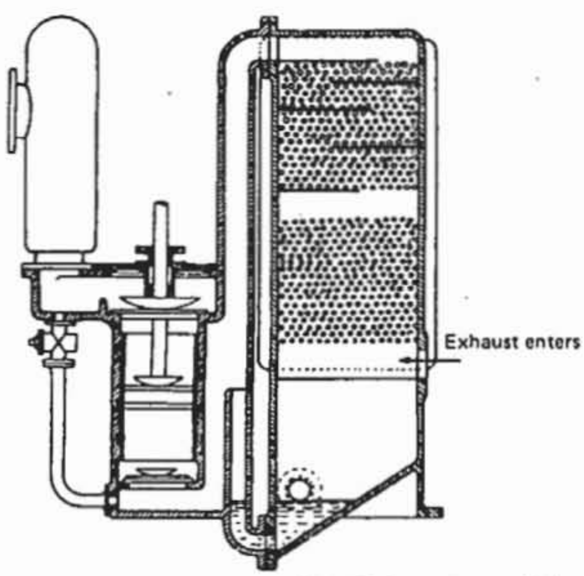

Figure 1 Patent drawing of the Weir condenser [1].

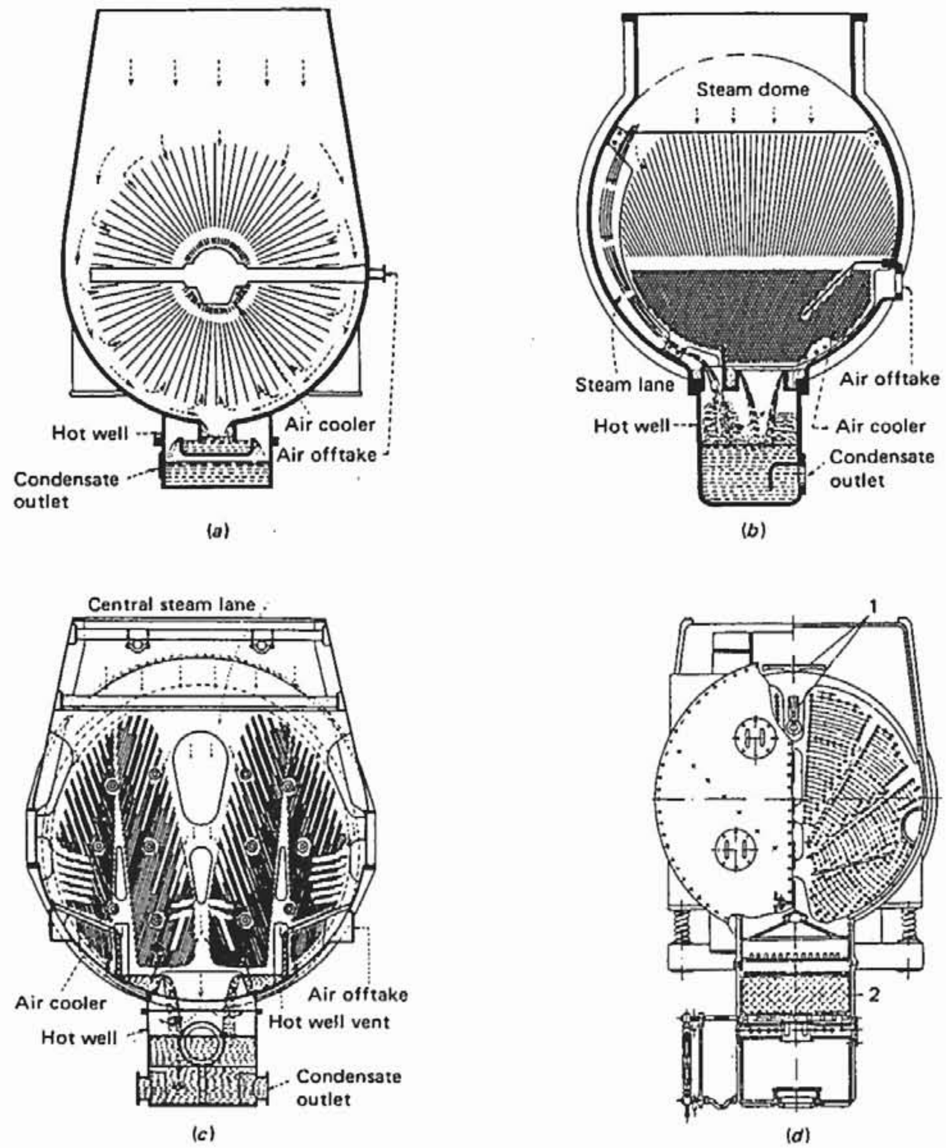

Figure 2 Various circular tube bundle geometries. (*a*) Eccentric radial bundle [6], (*b*) left-hand steam access lane [6]; (*c*) venturi-shaped central steam lane [6]; and (*d*) baffled, fan-type bundle [7].

tube bundle is located eccentrically to the shell so that steam may be distributed from the top around the sides with minimal flow resistance [6]. The steam flows radially inward in the tube bundle, which contains a central air cooler and air extraction point. Figure 2*b* shows a variation where a steam access lane is provided on the left-hand side of the bundle and the air cooler is located on the lower right [6]. Figure 2*c* shows a venturi-shaped central steam lane in a symmetric, folded-bundle arrangement with two separate air coolers [6]. Figure 2*d* shows a schematic arrangement of a fan type of bundle layout [7]. Each subbundle contains about 30 tubes with a gradual narrowing down of the steam flow passage along the steam flow direction. The subbundles are separated by baffle plates to remove condensate from above.

In each of these designs, numerous steam lanes are used to ensure that the steam is in close contact with the condensate at the bottom of the bundle. Also, the steam flow passages become narrower as the steam flows toward the air extraction point, in order to keep the vapor velocity large enough to ensure removal of noncondensable gases. A comprehensive review of the performance of several condensers in the United States was made by Chatel in 1927 [8]; it described the use of baffles near the air cooler, radial flow of steam, the use of steam lanes with eccentric shells, and condensate baffles. Emerson [9] postulated that an "ideal" bundle arrangement might be as shown in Fig. 3. It would have inlet steam guide vanes into the tube bundle to minimize the flow losses, radial flow of steam, generous access lanes, penetration of steam across a small number of tubes to minimize the bundle pressure drop, and a convergent air cooler passage to promote high velocities. Such a design would also put a large number of tubes in contact with fresh steam, making the condenser very effective. According to Emerson [9], high vapor velocities at the inlet to the condenser bundle may cause a large bundle pressure drop, which can affect subsequent thermal performance throughout the rest of the condenser. On the other hand, high velocities at the inlet to the air cooler help to promote large mass transfer coefficients, and the resulting pressure drop only influences the design of the air ejector equipment.

During the past 40 years, the construction of power plants with ever-increasing electrical capacities has required larger and larger condensers. In these large condensers, the cylindrical shell has been replaced with a rectangular one, and multiple-tube bundles with wider steam lanes have been developed. In the United States, it is commonplace to have radial-flow tube bundles with a central air cooler section [2], as shown in Fig. 4*a*. Elsewhere, a multifolded tube bundle arrangement, as shown schematically in Fig. 4*b*, is common [10–12]. The exact shape of the tube bundle varies with manufacturer, type of application, capacity, and so on, so that today condensers are built in many different sizes and shapes and with a variety of tube bundle configurations.

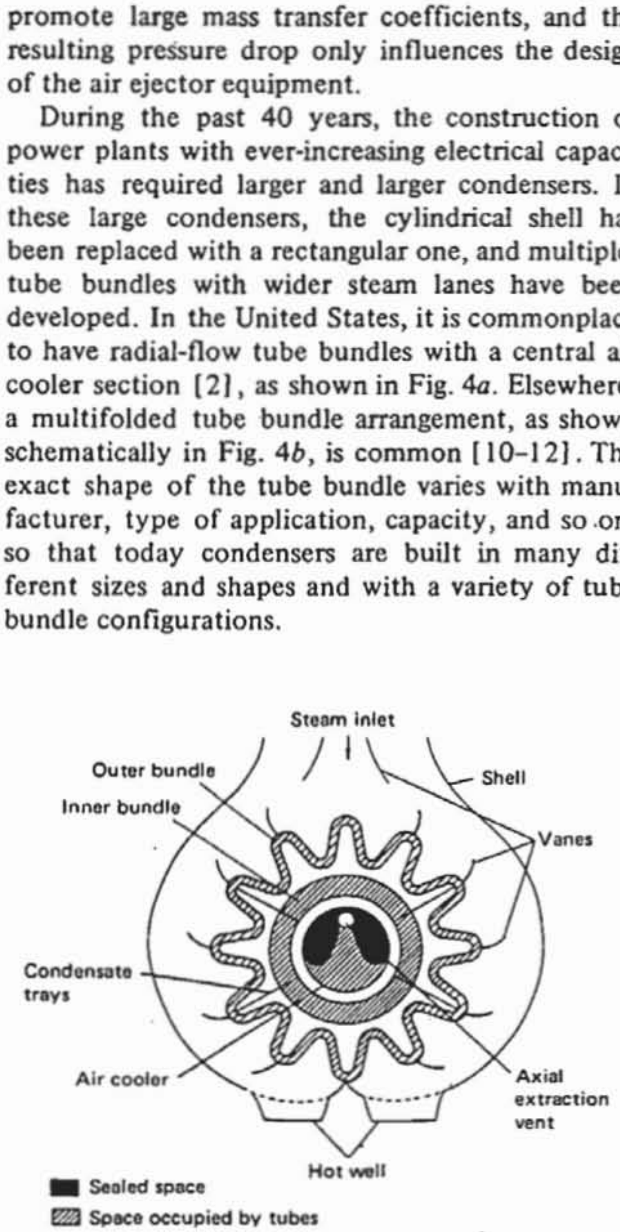

Figure 3 Section of ideal condenser bundle [9].

Current Thermal Design Practice

Most condensers today are thermally rated by standards similar to those proposed by the Heat Exchange Institute (HEI) in the United States [13] or the British Electrical and Allied Manufacturers' Association (BEAMA) [14]. These standards have been prepared with the supposition that the overall heat transfer coefficient in an operating condenser is proportional to the square root of the cooling water velocity and independent of steam-side conditions. This dependence on cooling water velocity has been the subject of various investigations for over 100 years and was addressed in the United States in 1910 by Orrok [15]. He conducted a series of tests for steam condensing on a single, horizontal tube having an outside diameter of 25.4 mm and a length of 1.16 m. He varied tube wall material and condenser operating vacuum, as well as cooling water velocity and inlet temperature. He also made a limited examination of the influence of corrosion, steam velocity, and air on single-tube performance.

Based on his early experimental results and a series of extensive tests subsequently conducted by HEI, the overall coefficient of heat transfer is postulated to be of the form:

$$U = CF_1F_2F_3\sqrt{v} \qquad (1)$$

where the coefficient C depends on tube outside diameter, and the other coefficients F_1, F_2, and F_3 are correction factors for fouling, tube material and wall thickness, and cooling water inlet temperature, respectively [13].

As might be expected, Eq. (1) is valid only over a limited velocity range where the cooling water thermal resistance controls the heat transfer process. If other thermal resistances (e.g., due to condensate, fouling, wall material or thickness, or noncondensable gases) are controlling, Eq. (1) may be in substantial error. For example, Wenzel [16] reported wide discrepancies between the predicted value of the overall coefficient from Eq. (1) (UHEI) and measured values from commercial condensers (UEXP) (Fig. 5). The comparison shows that in many cases HEI predictions may be too optimistic and errors of almost 100% are possible. Other data, however, show that some condensers perform better than predicted by HEI. These discrepancies are, of course, due to many factors, including air blanketing, maldistribution of flow on either the steam side or the cooling water side, condensate

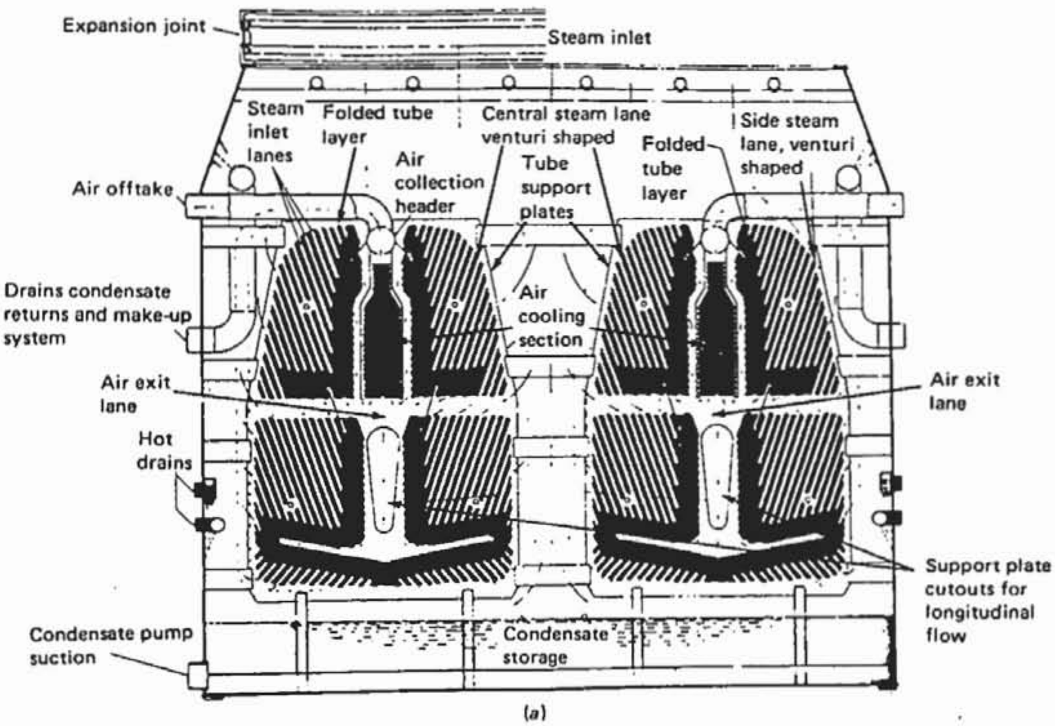

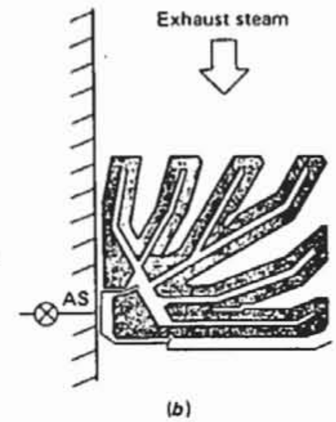

Figure 4 Noncircular bundle designs. (*a*) Multiple tube bundle design, Worthington [2]. (*b*) Multifolded tube bundle [10].

splashing on the tubes, high vapor velocity effects, dropwise condensation, poor experimental measurements, and others. It is clear that there is much room for improvement in present rating techniques.

The basic HEI procedure as described above has been criticized [17, 18] for failing to include all

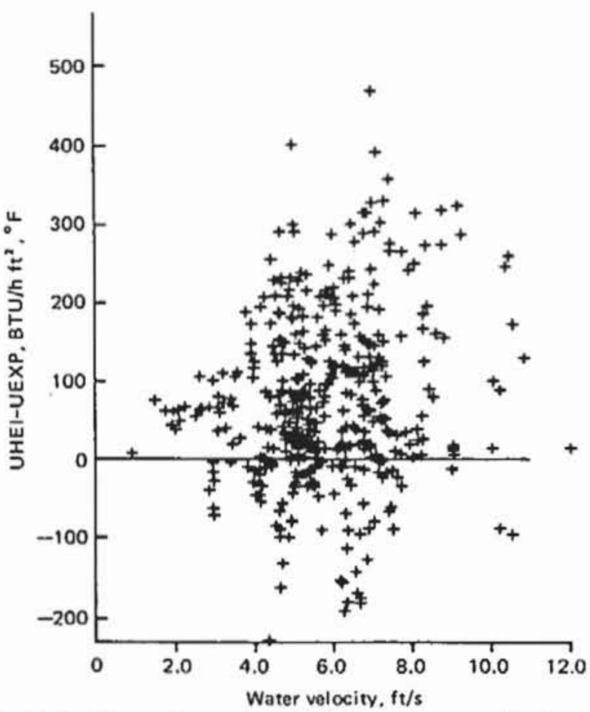

Figure 5 Comparison of predicted and measured values of overall heat transfer coefficient [16].

the thermal resistances between the vapor and the cooling water as given below:

$$\frac{1}{U_o} = \frac{1}{h_i}\frac{A_o}{A_i} + \frac{1}{h_o} + R_{nc} + R_w + R_f \tag{2}$$

Only when Eq. (2) is utilized locally will it be possible to perform more accurate analyses of condensers and improve their performance. In considering the use of Eq. (2), it is true that in most steam condensers today, with cooling water velocities of 1–3 m/s, the thermal resistance on the tube side is usually controlling. This is certainly true in regions of the condenser where vapor velocities are very large, leading to high steam-side coefficients. However, there may be other regions in a condenser where shell-side conditions are controlling (e.g., near the air cooler, where there are sizable noncondensable gas concentrations). In addition, there can be other important design situations where shell-side conditions control performance, such as the use of titanium tubes with higher cooling water velocities [19], the use of heat transfer tubing with high internal enhancements, or applications where an organic vapor, with its low condensing coefficient, is being condensed. Under these circumstances, it will be essential to more thoroughly understand and model shell-side phenomena.

Consideration of vapor pressure drop reveals another reason why shell-side conditions are important. As pointed out earlier, if an improvement can be made in condenser vacuum, the thermodynamic efficiency of the power cycle will increase, leading to savings in fuel costs. Unfortunately, a current problem with operating steam power condensers is their ability to achieve a high vacuum, and a vacuum shortfall of only about 0.5 kPa (0.15 in Hg) could produce an additional annual fuel cost of over $1 million for a 2000-MW plant [20]. As bundle geometries change, vapor velocities may become very large, causing undesirable pressure losses that can have a dramatic effect on performance, especially at low operating pressures. Table 1 compares the effects of vapor pressure drop for three different condenser operating pressures, 8.58, 6.76, and 5.10 kPa (2.5, 2.0, and 1.5 in Hg). The values were calculated for steam flowing radially inward in a 30° segment of a circular bundle containing 228 tubes in 22 rows. For a steam mass velocity of 0.618 kg/m² s, pressure drops of 0.39, 0.67, and 1.12 kPa occur. This threefold increase in pressure drop at the lower operating pressure causes a larger decrease in saturation temperature, which lowers the log mean temperature difference (LMTD) by almost one-half. The amount of steam condensed, m_c, is therefore lowered proportionately. It is also interesting to see that at lower condenser pressures, vapor velocities can become very large. At a pressure of 2.5 in Hg, the steam velocity decreases from 43.1 to 20.5 m/s from inlet to outlet. This reduction in steam velocity provides some pressure recovery, helping to keep the pressure drop small. At 2.0 in Hg the steam velocity stays essentially constant (actually, the velocity first decreases with penetration into the bundle, then increases toward the last rows). At 1.5 in Hg, because only half of the steam is condensed in comparison to the 2.5-in case, as the pressure of the steam drops its density becomes very small, requiring that the steam velocity increase by a factor of 2 from inlet to outlet. Such large velocities are undesirable and can lead to excessive tube vibration and premature failure [21, 22]. Uncertainties in pressure drop prediction may therefore have a serious effect on design performance, especially at lower operating pressures, and it becomes imperative to understand shell-side two-phase flow to avoid significant pressure losses.

Table 1 Effect of Operating Pressure on Condenser Performance[a]

Performance variables	Inlet steam pressure (in Hg)		
	2.5	2.0	1.5
$P_{s,i}$ (kPa)	8.48	6.76	5.10
$T_{s,i}$ (°C)	42.5	38.3	33.1
U_i (m/s)	43.1	53.3	68.0
U_e (m/s)	20.5	53.2	125.2
ΔP_s (kPa)	0.39	0.67	1.12
ΔT_s (°C)	0.76	1.68	4.08
LMTD (°C)	12.54	9.95	6.70
$\dot{m}_c$ (kg/s)	2.07	1.65	1.06

[a] Bundle geometry: 30° segment of circular bundle; Steam flow direction: radially inward; Number of tubes: 228; Number of tube rows: 22; Tube diameter: 15.9 mm; S/d: 1.35; Steam mass velocity, G: 0.618 kg/m² s.

SHELL-SIDE HEAT TRANSFER

In 1916 Nusselt conducted his pioneering analysis of laminar film condensation on a single horizontal tube [23]. He idealized the problem by assuming, among other things, a pure quiescent vapor and a uniform tube wall temperature. His analysis yielded the well-known relationship for the heat transfer coefficient:

$$h_N = 0.725 \left[\frac{k_L^3 h_{fg} \rho_L^2 g}{d_o \mu_L (T_s - T_w)} \right]^{1/4} \tag{3}$$

which can be expressed in dimensionless form:

$$\mathrm{Nu}_N = \frac{h_N d_o}{k_L} = 0.725 \left(\frac{\mathrm{Ga\,Pr}}{H} \right)^{1/4} \tag{4}$$

Numerous investigators have compared Eq. (3) with single-tube experimental data, using a variety of test fluids, and agreement within 30% has generally been obtained. During shell-side condensation in an actual condenser, however, the conditions are widely different from those used by Nusselt. Added complexities exist due to the presence of neighboring tubes in a large tube bundle [24–28]. If the situation is idealized as depicted in Fig. 6*a*, all the condensate from a given tube is assumed to drain by gravity to the lower tubes in a continuous, laminar sheet. In reality, depending on the spacing-to-diameter ratio of the tubes and depending on whether they are arranged in a staggered or in-line configuration, the condensate from one tube may not fall on the tube directly below it but instead may flow sideways (Fig. 6*b*). Also, it is well known experimentally

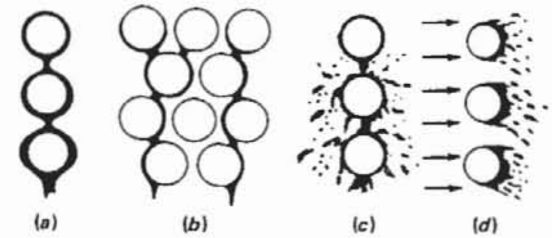

Figure 6 Schematic representations of condensate flow. (*a*) Nusselt idealized model; (*b*) side-drainage model; (*c*) ripples, splashing, and turbulence; and (*d*) high vapor cross flow.

that condensate does not drain from a horizontal tube in a continuous sheet but in discrete droplets along the tube axis. When these droplets strike the lower tube, considerable splashing can occur (Fig. 6*c*), causing ripples and turbulence in the condensate film. Perhaps most important of all, large vapor velocities can create significant shear forces on the condensate, stripping it away, independent of gravity (Fig. 6*d*).

The effects of vapor velocity and condensate inundation can therefore cause a significant change in shell-side condensation heat transfer and must be accurately accounted for in any valid condensation analysis. However, to proceed from the single-tube theory to a tube bank condensation model is a difficult process. Figure 7, which has been adapted from [25], outlines the important research work that is necessary to accomplish this goal, and provides a list of pertinent references [29–67, 71, 72] which have contributed significantly to the understanding of this subject.

Effect of Vapor Velocity

When the vapor surrounding a horizontal tube is moving at a high velocity, the analysis for film condensation is affected in two important ways: (1) the surface shear between the vapor and the condensate τ_i must be included (i.e., the local vapor flow field must be known), and (2) the effect of vapor separation—its onset and its subsequent influence on condensate flow—must be accurately treated. A further complicating feature occurs when it is realized that the vapor flow direction in an operating condenser may be oriented in a variety of ways with respect to gravity. This last characteristic introduces an asymmetry into the problem which further complicates the analysis. As a result, most of the analyses performed to date have been for vertical downflow

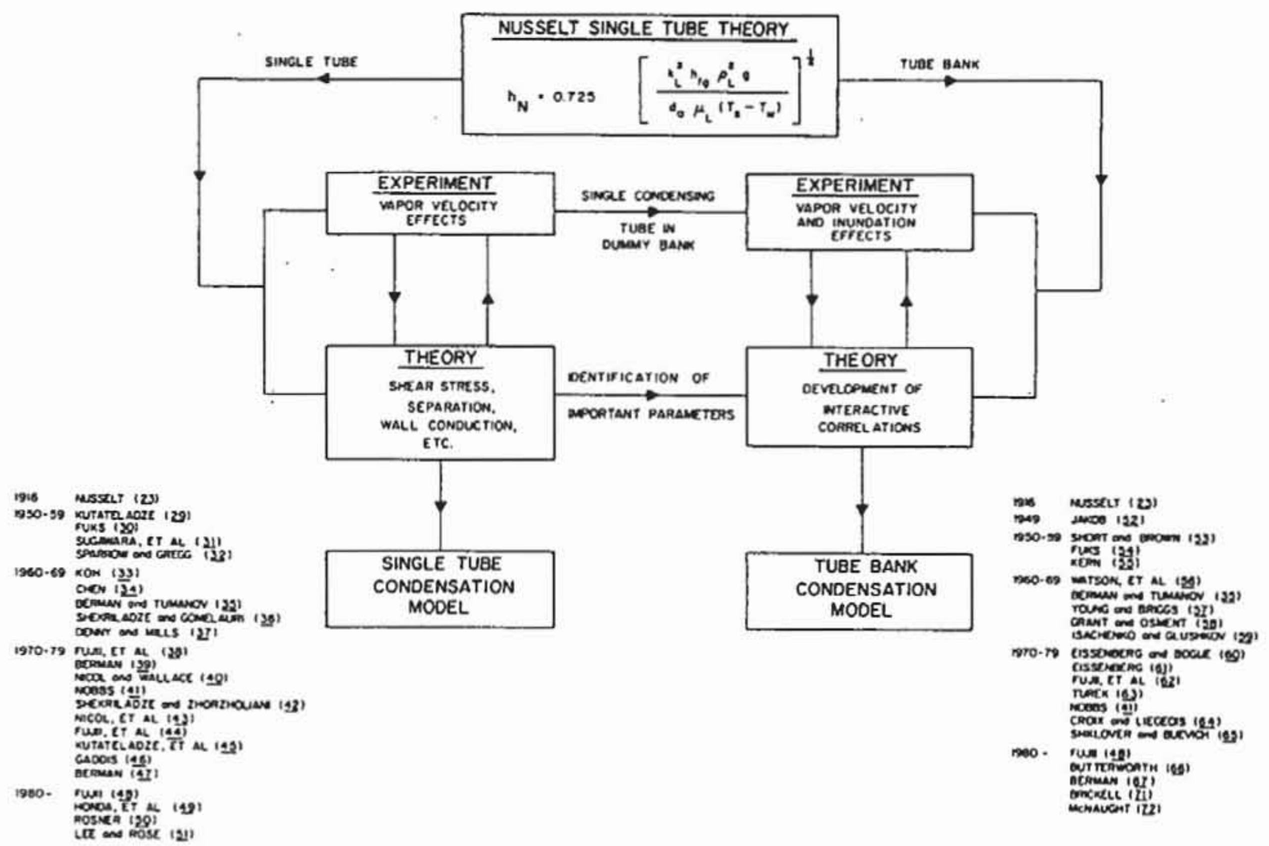

Figure 7 Outline of research on vapor condensation without noncondensables [25].

of vapor. An excellent overview of the effect of vapor velocity was recently made by Lee and Rose [51].

Experimental results [30, 35, 41] have shown that by increasing the vapor velocity, the condensing heat transfer coefficient can be significantly increased. Berman and Tumanov [35] conducted a series of experiments on a single horizontal tube placed in a bank of uncooled neighboring tubes. They recommended that for vertical downflow, the increase in heat transfer coefficient may be expressed in terms of the vapor Reynolds number Re_v and the heat flux (i.e., Nu_N):

$$\frac{h}{h_N} = 1 + 9.5 \times 10^{-3} (Re_v)^{11.8/\sqrt{Nu_N}} \tag{5}$$

provided

$$(Re_v)^{11.8/\sqrt{Nu_N}} < 50$$

The early analytical investigations with vapor velocity effects were extensions of Nusselt's analysis to include the interfacial shear boundary condition at the edge of the condensate film:

$$\tau_i = C_f \frac{\rho_v U_\infty^2}{2} \tag{6}$$

Initially, the friction coefficient C_f was assumed constant, but later this restriction was relaxed to allow C_f to be a function of vapor Reynolds number [29–31, 35]. These authors also assumed that the interfacial shear during condensation was the same as that which occurs when a noncondensing gas flows over a dry surface. This erroneous approach was correctly identified by Shekriladze and Gomelauri [36], who realized that the mass flow across the condensing interface is very important. They therefore assumed that the primary contribution to the surface shear was due to the change in momentum across the interface:

$$\tau_i = j(U_\phi - u_i) \tag{7}$$

They also simplified the problem by assuming $u_i \ll U_\phi$ with U_ϕ provided from potential flow theory. Their approximate solution for an isothermal cylinder without separation and with no body forces is:

$$Nu = \frac{h d_o}{k_L} = 0.9\, Re_{2\phi}^{1/2} \tag{8}$$

where $Re_{2\phi}$ is a two-phase Reynolds number, defined by $U_\infty \rho_L d_o / \mu_L$. When both gravity and velocity are included, they recommended the relationship:

$$\frac{Nu}{Re_{2\phi}^{1/2}} = 0.64[1 + (1 + 1.69F)^{1/2}]^{1/2} \tag{9}$$

where

$$F = \frac{Pr}{Fr\, H} = \frac{g d_o \mu_L h_{fg}}{U_\infty^2 k_L (T_s - T_w)} \tag{10}$$

It is interesting to note that in the limiting case of zero vapor velocity (i.e., $F \to \infty$), Eq. (9) reduces to the Nusselt expression given by Eq. (4). Equation (9) neglects vapor separation, and at high vapor velocities it is well known that for flow over a cylinder, separation will occur somewhere between 82° and 180° from the stagnation point of the tube. When separation occurs, the condensate film rapidly thickens downstream of the separation point and, as a result, heat transfer is deteriorated. A conservative approach suggested by Shekriladze and Gomelauri [36] is to assume that there is no heat transferred beyond the separation point. If the minimum separation angle of 82° is then chosen, the most conservative equation results. With these assumptions, the heat transfer will decrease by approximately 35%. An interpolation formula based on this conservative approach, which satisfies the extremes of gravity- and velocity-dominated condensate flow, was recently proposed by Lee and Rose [5]:

$$\frac{Nu}{Re_{2\phi}^{1/2}} = 0.416[1 + (1 + 9.47F)^{1/2}]^{1/2} \tag{11}$$

They pointed out that Eq. (11) is conservative in three ways: the assumed shear stress is less than the actual shear stress, so the condensate film near the top of the tube should be thinner; the separation angle of 82° is less than the actual separation angle; and, beyond the separation point, the heat transfer rate is finite and nonzero.

More recent complete analyses by Fujii and coworkers [38, 44, 48, 49] have considered details of the vapor boundary layer, variations in the separation point, circumferential conduction effects in the tube wall, and vapor velocities oriented away from the vertical. Their earliest work for downflow of vapor over an isothermal cylinder resulted in an approximate formula that satisfies both limiting cases of large and small vapor velocities [38]:

$$\frac{\mathrm{Nu}}{\mathrm{Re}_{2\phi}^{1/2}} = X\left(1 + \frac{0.276F}{X^4}\right)^{1/4} \tag{12}$$

where

$$X = 0.9(1 + G^{-1})^{1/3} \tag{13a}$$

and

$$G = \frac{(T_s - T_w)k_L}{\mu_L h_{fg}}\left(\frac{\rho_L \mu_L}{\rho_v \mu_v}\right)^{1/2} \tag{13b}$$

Lee and Rose [51] conservatively modified the expressions above by neglecting heat transfer downstream of the calculated separation point. They recommended the following expression:

$$\frac{\mathrm{Nu}}{\mathrm{Re}_{2\phi}^{1/2}} = \zeta\left(1 + \frac{0.281F}{\zeta^4}\right)^{1/4} \tag{14}$$

where

$$\zeta = 0.88\left(1 + \frac{0.74}{G}\right)^{1/3} \tag{15}$$

Equation (14) approaches the Nusselt solution, Eq. (4), when $U_\infty \to 0$ (i.e., $F \to \infty$). Both Eqs. (11) and (14) are plotted, together with experimental data, in Fig. 8 [51]. Except for the data at very high vapor velocities (i.e., very low F), all the data lie above the prediction of Eq. (11), verifying its conservative nature. Equation (14) correlates the data fairly well for various values of G. It is apparent, however, that more experimental data are needed for low values of F (i.e., large U_∞) and small values of G (i.e., low heat flux) in order to verify the dependence on G.

Effect of Condensate Inundation

In the absence of vapor velocity, as condensate flows by gravity onto lower tubes in a bundle, the condensate thickness around a tube should increase, and the condensate heat transfer coefficient should therefore decrease.

Jakob [52] extended the Nusselt analysis for film condensation heat transfer on a vertical in-line row of horizontal tubes. In this idealized case (Fig. 6a) it is assumed that all the condensate from a given tube drains as a continuous sheet directly onto the top of the tube below it in a smooth laminar film. With this assumption, together with the assumption that the saturation temperature difference $(T_s - T_w)$ remains the same for all the tubes, Jakob showed that the average coefficient for a vertical row of n tubes, compared to the coefficient for the first tube (i.e., the top tube in the row), is:

$$\frac{\bar{h}_n}{h_1} = n^{-1/4} \tag{16}$$

or, in terms of the coefficient for the nth tube,

$$\frac{h_n}{h_1} = n^{3/4} - (n-1)^{3/4} \tag{17}$$

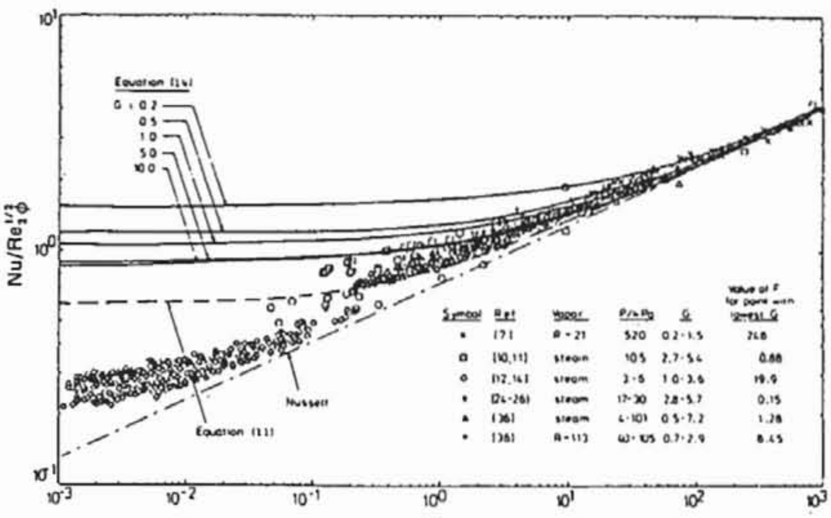

Figure 8 Effect of vapor velocity: a comparison of theory and experiment [51].

Kern [55] realized that the condensate does not drop off in a continuous sheet, but drops off instead by discrete droplets or jets of liquid depending on the surface tension of the condensate. These droplets cause ripples in the condensate film (Fig. 6*c*), and this disturbance of the film lessens the inundation effect. He therefore proposed a less conservative relationship:

$$\frac{\bar{h}_n}{h_1} = n^{-1/6} \tag{18}$$

or

$$\frac{h_n}{h_1} = n^{5/6} - (n-1)^{5/6} \tag{19}$$

Chen [34] derived a modified Nusselt expression, which considered the additional effects of the momentum gain of the falling condensate and the condensation of vapor on the subcooled condensate sheet between tubes. As a result, he arrived at an approximate expression that is valid for most ordinary applications:

$$\frac{\bar{h}_n}{h_1} = n^{-1/4}[1 + 0.2H(n-1)] \tag{20}$$

provided $H(n-1) \leqslant 2.0$. Eissenberg [61] experimentally investigated the effects of condensate inundation by using a test bundle containing 163 tubes in a tightly spaced ($s/d = 1.33$), staggered arrangement. Based on his observations, he postulated that condensate does not always drain onto tubes aligned vertically but instead can be diverted sideways (due to local vapor flow conditions) to follow a staggered path similar to that shown in Fig. 6*b*. Assuming a gravity-dominated situation, he theorized that in this side drainage mode the condensate strikes the lower tubes on their sides rather than their tops, and the inundation influences the condensate flow only on the bottom portions of the tubes, which carry away less heat than the tops. For this situation, he subsequently derived an expression that predicts a minimum effect of inundation:

$$\frac{\bar{h}_n}{h_1} = 0.60 + 0.42n^{-1/4} \tag{21}$$

Numerous experimental measurements have been made in studying the effect of condensate inundation [41, 53, 54, 56–61]. In general, however, the data are very scattered, giving the result depicted in Fig. 9. Recall that the Nusselt expression as derived by Jakob, Eq. (16), predicts the most conservative effect, whereas the side drainage model of Eissenberg, Eq. (21), is least conservative. The data show considerable scatter around each of these theoretical expressions. Recently, Berman [67] conducted a comprehensive compilation of film condensation data on bundles of horizontal tubes. Figure 10 shows some of the data he considered. In Fig. 10, *a–c*, the data of Ferguson and Oakden [68] and Gudemchuk [69] for experiments with multirow, staggered tube bundles are plotted. The top curves depict the falloff of the local coefficient h_n in relation to the coefficient for the first tube in the row, h_1. The bottom curves depict the falloff in relation to the Nusselt expression h_N, Eq. (3). The data of [69] show that as steam flow rate (i.e., steam velocity) through the bundle decreases, a significant erroneous dropoff occurs in h_n/h_1 (Fig. 10, *b* and *c*, curves 4 and 5) as the amount of steam is used up in going through the earlier tubes in the bundle. Furthermore, it is evident that near the top of the bundle h_n/h_N is greater than unity, signifying that, due to high steam velocities, the heat transfer coefficient increases above the Nusselt value. With penetration into the bundle, the local heat transfer coefficient falls off not only due to inundation but, more important, due to a decreasing local steam velocity. Hence, all bundle data will have a mixture of inundation and vapor velocity effects, which are difficult to separate from one another. Figure 10*d* shows the results of Nobbs [41], who used one active tube in a dummy tube bundle. He simulated additional condensate from above by using three porous tubes supplied with water. In this figure, the top curves depict h_Y/h_1 and the lower curves

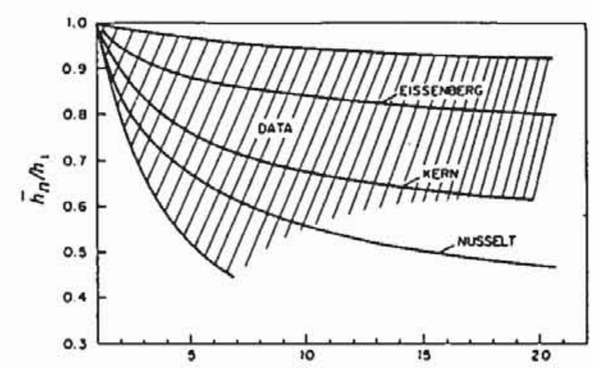

Figure 9 Schematic representation of the uncertainty between theory and experiment during condensate inundation studies.

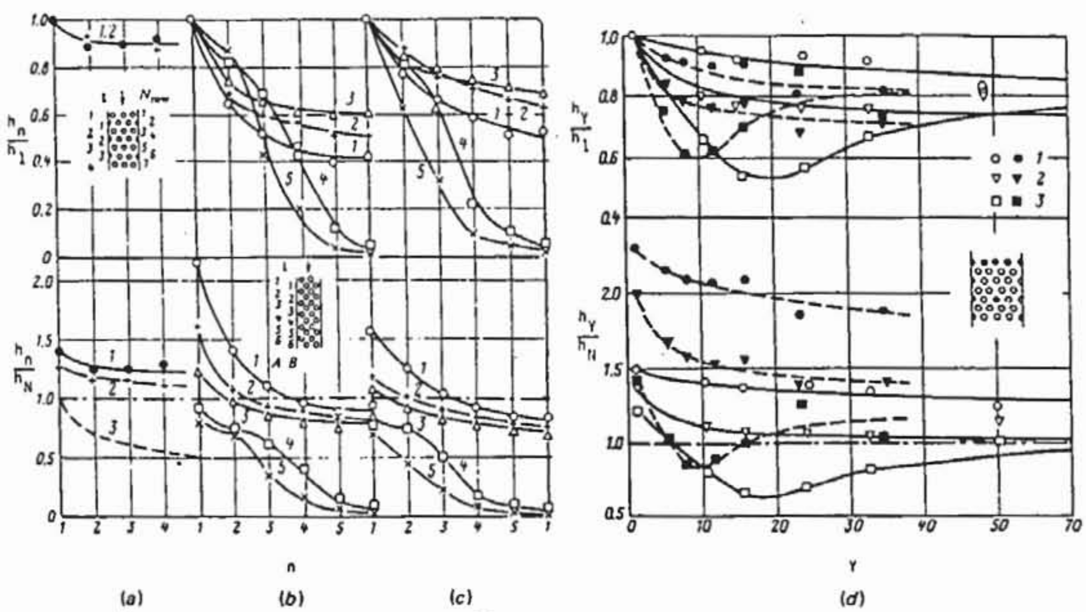

Figure 10 (*a*) Data from [68]: $T_s = 48.9°C$, (1) $U = 50.7$ m/s, (2) $U = 24.3$ m/s, (3) $U = 0$ (i.e., Nusselt); (*b*) and (*c*) Data from [69]: $T_s = 97–112°C$, (*b*) Row A, (*c*) Row B, (1) $U = 26.3$ m/s, (2) $U = 19.4$ m/s, (3) $U = 13.6$ m/s, (4) $U = 6.4$ m/s, (5) $U = 4.5$ m/s; and (*d*) Data from [41]: $T_s = 101.5°C$, Solid curve: cooling water inlet = 68.5°C. Dashed curve: cooling water inlet = 36.5°C. (1) $U = 48.6$ m/s, (2) $U = 27$ m/s, (3) $U = 5.4$ m/s.

depict h_Y/h_N, where h_Y is the heat transfer coefficient corresponding to the local value of inundation Y, where Y equals $(\Sigma G)_n/G_n$ [$(\Sigma G)_n$ equals the total flow of condensate per unit area running off the nth tube and G_n equals the flow of condensate per unit area forming on the nth tube]. Again, the wide scatter in the data is evident, as noted earlier, and depends on heat flux (in this case, steam-to-cooling water temperature difference) and steam velocity. At low steam velocities, the data appear to go through a minimum, perhaps signifying that for very large amounts of condensate, considerable splashing occurs, leading to turbulence in the condensate film. Based on this information, Berman [67] concluded that the wide variation in experimental data for tube bundle inundation is due to many variables, such as bundle geometry (in-line or staggered), tube spacings, type of condensing fluid, operating pressure, heat flux, local vapor velocity, and, of course, the difficulties in attempting to measure directly, or indirectly, the local condensing coefficient.

The comparison above was made for vertical downflow of vapor. If one allows the vapor flow direction to vary, additional complexities are introduced. Figure 11 compares the data of Fujii [48] for both in-line and staggered tube bundles with steam flowing downward, horizontally, or upward. There is little difference between the downward and horizontal flow data, whereas the upward flow data are as much as 50% lower in the range $0.1 < F < 0.5$, and are even less than the single-tube, zero-velocity, Nusselt expression, Eq. (4). The solid curve in Fig. 11 is an approximate expression given by Fujii [48]:

$$\frac{\mathrm{Nu}}{\mathrm{Re}_{2\phi}^{1/2}} = 0.96F^{0.2} \tag{22}$$

for $0.03 < F < 600$.

Hawes [70] obtained some data for horizontal cross flow which showed that as vapor velocity increases, the heat transfer coefficient first increases and then decreases. This maximum is presumably due to a critical vapor velocity being reached where condensate holdup occurs locally around a tube due to hydrodynamic conditions. This trapping of condensate leads to thicker condensate films on the tubes and a deterioration in performance. Butterworth [26] suggested that since the Hawes data were obtained at high vapor velocities and low heat fluxes (i.e., low temperature differences between the vapor and the cold wall), the observed results could be interpreted differently. Butterworth postulated that at very high vapor velocities, the local drop in vapor pressure around a tube can cause a reduction in local saturation temperature, which reduces the heat transfer driving force. He therefore suggested that to avoid a decrease in heat transfer with an increase

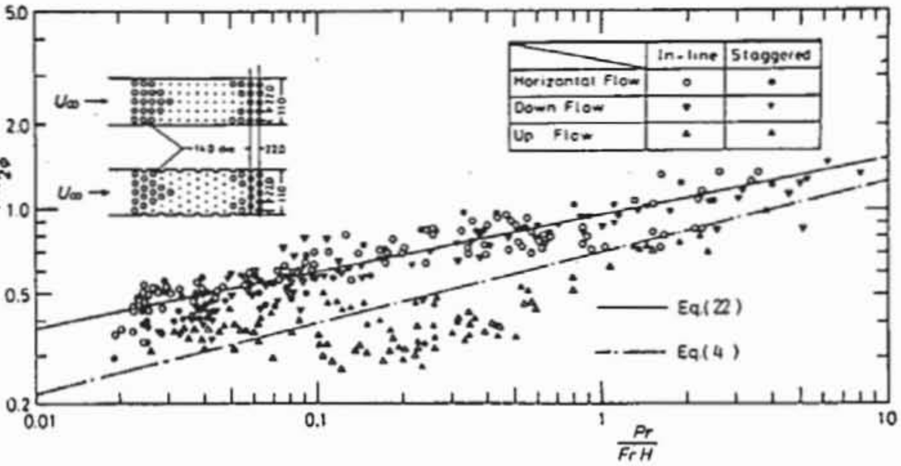

Figure 11 Correlation of theory and experiment for horizontal, downward, and upward flow in tube bundles [48].

in vapor velocity, the ratio of the local vapor temperature drop to the local film temperature difference should be kept small, that is, $(T_s U_v^2 / h_{fg}) / (T_s - T_w) \leq 0.05$. Brickell [71] further discussed this issue of condensate holdup and pointed out that if a general inundation expression is desired of the form:

$$\frac{\bar{h}_n}{h_1} = \left[\frac{(\Sigma\, G)_n}{G_n} \right]^{-s} \tag{23}$$

then the exponent s will not be constant but will vary with vapor velocity, flow direction, and pitch-to-diameter ratio, as shown in Fig. 12. He further postulated that the condensate should be treated as having two components, a film flow and a drop flow, with droplet entrainment occurring due to local vapor velocity conditions. From this information, it is evident that there is a substantial interactive effect between vapor shear and condensate inundation, and these effects cannot be treated independently.

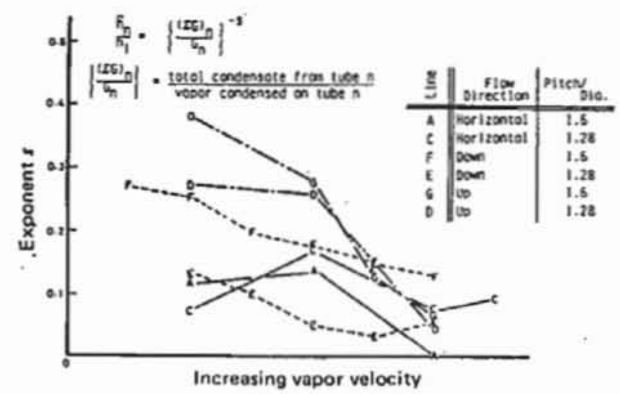

Figure 12 Effects of vapor velocity, flow direction, and tube spacing on inundation exponent [71].

Combined Vapor Shear and Inundation

Until recently, the effects of vapor shear and inundation were treated separately, based on the assumption that there is little interaction between these physical phenomena. The combined average heat transfer coefficient for shell-side condensation with n tubes in a vertical row was written as

$$\bar{h}_n = h_N C_n C_v \tag{24}$$

where C_n is a correction to the single-tube Nusselt expression to take into account condensate inundation, and C_v is a correction for vapor velocity effects.

Grant and Osment [58] proposed the following expression:

$$\bar{h}_n = h_N \left[\frac{(\Sigma\, G)_n}{G_n} \right]^{-0.223} (1 + 0.0095\, \mathrm{Re}_v^{11.8/\sqrt{\mathrm{Nu}_N}}) \tag{25}$$

which is a combination of Eqs. (5) and (23). Equation (25) correlated their experimental data with a root-mean-square deviation of 13%. Butterworth [26] recommended the relationship:

$$\bar{h}_n = n^{-0.16} [\tfrac{1}{2} h_{sh}^2 + (\tfrac{1}{4} h_{sh}^4 + h_N^4)^{1/2}]^{1/2} \tag{26}$$

where h_{sh} is the coefficient predicted by Shekriladze and Gomelauri [36] at high velocity [Eq. (8)] multiplied by 0.66 to conservatively account for the effect of separation. Butterworth [26] further suggested that in the expression above, the vapor velocity within the tube bundle should be calculated by dividing the velocity with no tubes present by the void fraction of the bundle. Based on the earlier information described in this paper, another expression that should be valid would be a combination of Eqs. (14) and (23):

$$\bar{h}_n = \left[\frac{(\Sigma\, G)_n}{G_n}\right]^{-s} \frac{k_L}{d_o} \mathrm{Re}_{2\phi}^{1/2} \zeta \left(1 + \frac{0.281F}{\zeta^4}\right)^{1/4} \tag{27}$$

where the exponent s is an empirical constant obtained from Fig. 12 and ζ is given by Eq. (15).

Recently, McNaught [72] pointed out that the relationships above all neglect the interactive effects of vapor shear and inundation, and suggested that shell-side condensation at high vapor velocities might be treated as two-phase forced convection. He therefore assumed that high vapor velocity data may be correlated by an expression of the form:

$$\frac{h_{2\phi}}{h_L} = a\left(\frac{1}{X_{tt}}\right)^b \tag{28}$$

where h_L is the liquid-phase forced-convection coefficient across a bank of tubes, and X_{tt} is the Lockart-Martinelli parameter given by:

$$X_{tt} = \left[\left(\frac{1-x}{x}\right)^{1.8}\left(\frac{\rho_v}{\rho_L}\right)\left(\frac{\mu_L}{\mu_v}\right)^{0.2}\right]^{1/2} \tag{29}$$

He then correlated the data of Nobbs [41] for steam with both staggered and in-line tube bundles and found that reasonable agreement was obtained for $a = 1.26$ and $b = 0.78$, so that for shear-controlled condensation Eq. (28) may be assumed to be valid. For gravity-controlled condensation he used

$$h_{gr} = h_N \left[\frac{(\Sigma\, G)_n}{G_n}\right]^{-s} \tag{30}$$

where s equals 0.22 for an in-line bundle and 0.13 for a staggered bundle. He added each contribution to get:

$$\bar{h}_n = (h_{sh}^2 + h_{gr}^2)^{1/2} \tag{31}$$

where h_{sh} is given by Eq. (28) and h_{gr} by Eq. (30), and found that about 90% of the data could be predicted to within ±25% by this two-phase multiplier method. Clearly, there is a need to obtain additional data in tube bundles under carefully controlled and observed conditions, and to further study two-phase forced-convection data for different fluids in various tube bundles to ascertain whether such a method has more general potential.

Accurate measurements of steam-side coefficients in large, operating power condensers are very difficult to obtain, and only limited data have been reported in the literature [7, 73–76]. Nevertheless, with new measurement techniques [77] and the proper selection of instrumented tubes in large tube bundles, very valuable information can be gathered on condensate inundation and vapor velocity effects. Accurate, large-scale bundle tests, though costly, will continue to be needed for some time.

Effect of Noncondensable Gases

It is well known that in the presence of a small amount of noncondensable gas, condensation heat transfer rates may be significantly reduced. In this situation, an added thermal resistance exists, since the vapor molecules must diffuse through a gas layer in order to reach the cold surface. Excellent summaries of this phenomenon, including reviews of the pertinent heat and mass transfer relationships, were recently made by Chisholm [78] and Webb and Wanniarachchi [79].

The procedure most widely used to calculate shell-side heat transfer in this situation is due to Colburn and Hougen [80]. They proposed a point-by-point, trial and error method that requires equating the heat transferred locally through the condensate, tube wall, and cooling water film to the sum of the sensible heat transferred by cooling the noncondensable gas and the latent heat deposited on the condensate film due to the amount of vapor transferred by diffusion. Variations of this method have been proposed and verified by experiment [61, 81, 82]. An important part of this method is the requirement of knowing the mass transfer coefficient for the diffusion of the vapor through the vapor-gas mixture. This term is evaluated by using the heat and mass transfer analogy together with empirical data for forced-convection gas-side heat transfer. Berman and Fuks [83], however, obtained an empirical expression for the mass transfer coefficient in a tube bundle during downward flow of a steam-gas mixture. This correlation has also been shown to be valid for horizontal flow [84]. Their expression can be used to generate an equivalent, noncondensable gas heat transfer coefficient [25, 78]:

$$h_{nc} = \frac{aD}{d_o} \mathrm{Re}_v^{1/2} \left(\frac{P_m}{P_m - P_v}\right)^b P_m^{1/3} \left(\frac{\rho_v h_{fg}}{T_v}\right)^{2/3} \times \frac{1}{(T_v - T_s)^{1/3}} \tag{32}$$

where for $\mathrm{Re}_v > 350$,

$b = 0.6$	$a = 0.52$	first tube row
	$a = 0.67$	second tube row
	$a = 0.82$	third and later tube rows

and for $\mathrm{Re}_v < 350$ [78],

$b = 0.7$	$a = 0.52$	all tube rows

Numerical solutions to the complete boundary-layer equations for condensation heat transfer in the presence of noncondensable gases also exist [85, 86], but the results are for flat plates and single tubes and are not generally useful. Recently, Rose [87, 88] proposed an approximate, but theoretically oriented, equation for forced-convection condensation on a single horizontal tube in the presence of a noncondensable gas. An analogy was made between condensation and flow normal to a cylinder with suction, and an approximate solution yielded the following result for the condensation mass flux in terms of the vapor Reynolds number, Schmidt number, and weight fraction of noncondensable gas:

$$\left(\frac{j}{\rho U_\infty}\right) \mathrm{Re}_v^{1/2} = \frac{\{1 + 2.28\,\mathrm{Sc}^{1/3}\,[(w_i - w_\infty)/w_\infty]^{1/2}\} - 1}{2\,\mathrm{Sc}} \tag{33}$$

The equation above was shown to be in good agreement with experimental data for steam-air, steam-hydrogen, Freon 113-air, and Freon 113-hydrogen [88].

Recently, Standiford [89] studied the effect of noncondensable gas on condenser heat transfer. He utilized the earlier data of Meisenburg et al. [90] for steam-air, which he claimed came closest to duplicating conditions in a normal condenser, and arrived at a very simple, though very approximate, correlation for the noncondensable gas resistance as a linear function of the weight fraction of air: $R_{nc} \simeq 0.004w$ $\mathrm{m^2\,K/W}$. This relationship will give conservative results since the Meisenburg data were obtained at low steam velocities (< 2 m/s), and Eqs. (32) and (33) show a square-root dependence on velocity. Since in most steam power condensers, the air-to-steam ratio is approximately 0.0001 at the turbine exhaust and 0.01 at the air cooler section [10], it is easy to see that the noncondensable gas resistance is of most importance where gas pockets are allowed to accumulate.

Proper condenser design should therefore allow for a well-defined vapor-gas flow path to avoid stagnation regions where the gas concentration can build up and retard heat transfer. It is also very important to design for the correct location of vents as well as for suitable steam access lanes [78, 89]. Coit [91] points out that improper design affects not only heat transfer but also corrosion due to excess O_2 absorption in the condensate when large gas pockets exist and temperatures fall off. Figure 13 shows schematically how design of the tube bundle can influence condenser performance [92]. Figure 13*a* shows an improperly designed four-pass condenser bundle having an air cooler section between each of the top and bottom tube bundles and a central steam access lane. The left portion of the figure shows an air-blanketed region (hatched circle) near the entrance to the air cooler. The right portion shows isotherms of the cooling water temperature rise. Notice that the heat transfer rate is fairly uniform in the top tube bundle as steam flows downward across the tubes. In the bottom bundle, however, performance rapidly drops off in the region of the gas pocket. Figure 13*b* shows an improved version of this condenser where the vertical partition plates were largely removed and the air cooling sections were partially opened to allow more steam to flow horizontally into the bundles. Care must therefore be exercised in designing the tube sheet layout, in locating the air vents, and in selecting properly matched air removal equipment [91].

Enhanced Heat Transfer

In recent years, numerous studies have been conducted on ways to enhance heat transfer [93–96]. Webb [97] provided an excellent review of enhancement methods for particular use in condensers, and several very recent studies have focused on the particular case of shell-side enhancement [98–100]. During shell-side condensa-

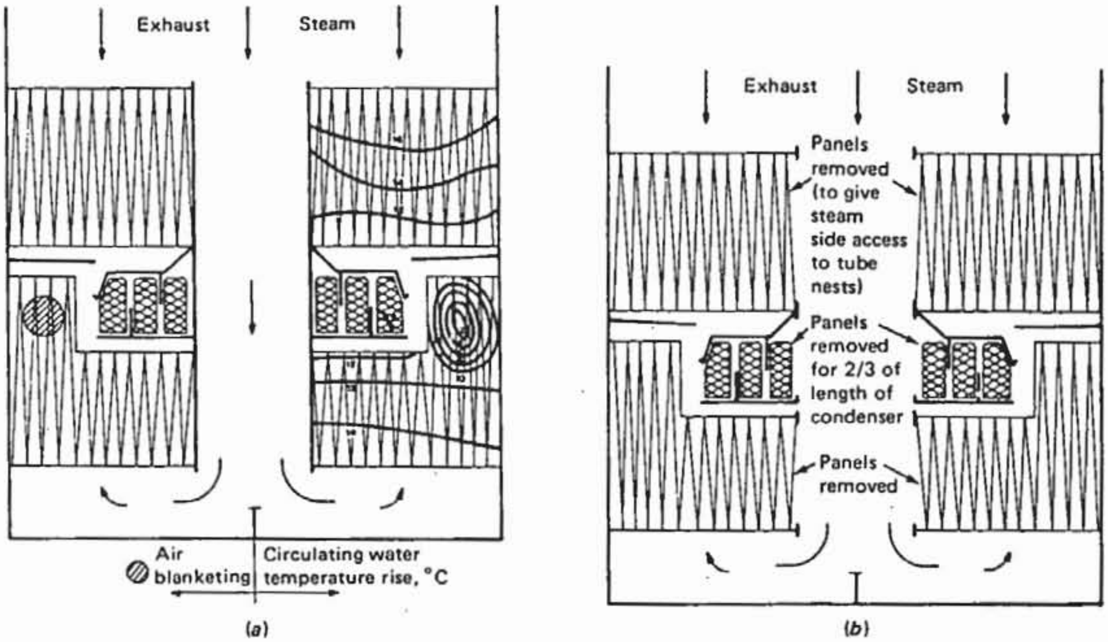

Figure 13 Modifications to improve air blanketing in a multibundle condenser [92]. (*a*) Before modifications; (*b*) after modifications.

tion a large thermal resistance occurs due to conduction of heat across the condensate film, and whatever can be done to thin or disturb this film is generally beneficial to heat transfer. For horizontal condenser tubes, this thinning may occur by promoting dropwise conditions (Fig. 14*a*); by using finned, grooved, or fluted surfaces (Fig. 14*b–d*); or by improving condensate drainage.

A review of dropwise condensation was made by Tanasawa [101], who discussed methods of promoting dropwise conditions. He stated that finding how to promote dropwise conditions for long periods of time was one of the most important problems to be solved before this mechanism can be practically applied. He further concluded that, of all the promoting techniques, the use of a thin coating of organic polymer (such as Teflon) was the most promising with respect to economic feasibility. With this technique, however, two major problems must be addressed: (1) organic coatings have poor thermal conductivities and must therefore be applied in the form of an ultrathin film in order to reduce their conduction resistance, and (2) techniques must be developed to apply these ultrathin films so that they strongly adhere to the condenser tube and have the toughness to withstand industrial conditions during assembly and use. Various investigations have been conducted with organic coatings on horizontal tubes, and enhancements as large as 180% have been measured [102]. In addition, in recent years significant advances have been made in the coatings industry, including the development of techniques for producing strongly adherent ultrathin films of organic materials for wear and lubrication [103]. With several of these new types of coatings, it may be possible to apply an ultrathin continuous film that has strongly adherent qualities. In so doing, long-lasting heat transfer improvements of several hundred percent may become a reality.

Since the early work of Beatty and Katz [104], the use of externally finned horizontal tubes in surface condensers has received much attention, although most of the efforts have been devoted to condensing refrigerants [105–109]. As originally described by Gregorig [110], the fins generate surface tension forces, which tend to thin the condensate film on the convex tips of the fins and to thicken the film in the concave channels, or troughs, between fins. In so doing, the condensing heat transfer coefficient has been enhanced by as much as 200% for steam [105], and by as much as 400% for refrigerants [107]. The use of a porous metal coating on a finned surface with Freon 113 enhanced the condensing heat transfer conductance (per unit length of tube) by more than 10 times [108]. Arai et al. [109] have shown that there is an optimum number of fins per meter, based on their data taken with Freon 12. Several theoretical investigations [111–113] show that, in addition to groove spacing, variables such as wall material, fin shape, and groove or trough dimensions are all

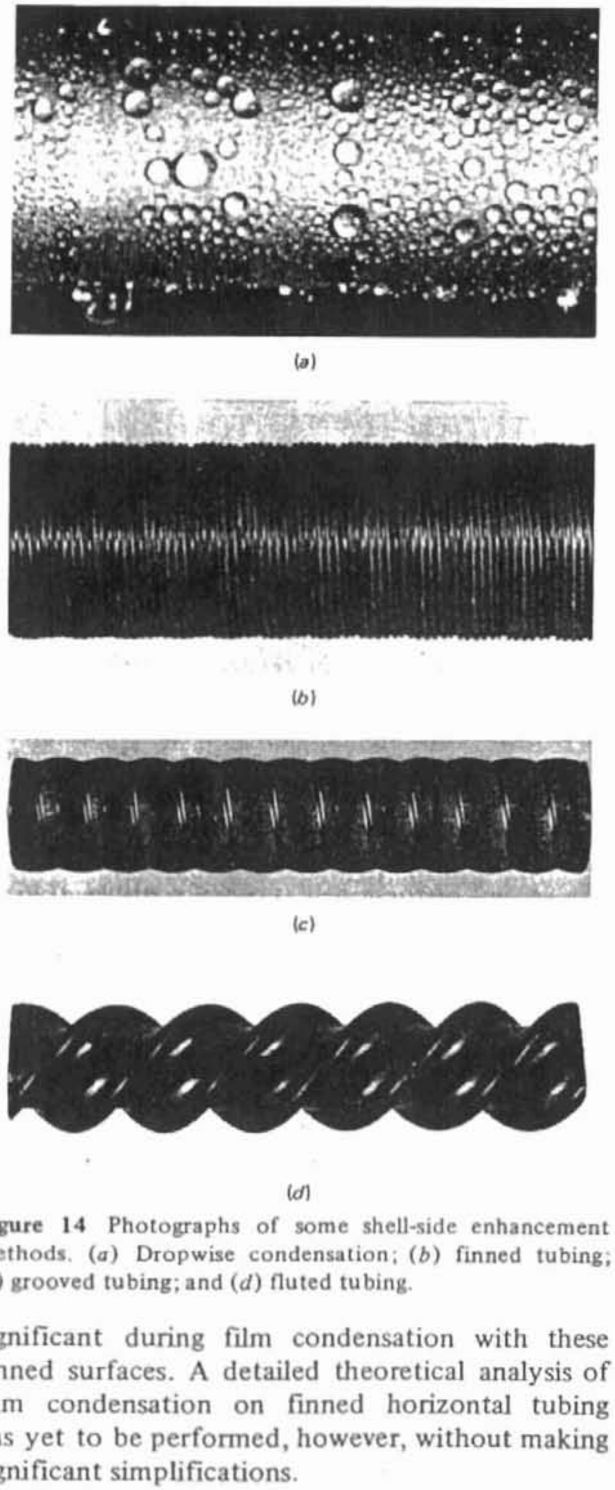

Figure 14 Photographs of some shell-side enhancement methods. (*a*) Dropwise condensation; (*b*) finned tubing; (*c*) grooved tubing; and (*d*) fluted tubing.

significant during film condensation with these finned surfaces. A detailed theoretical analysis of film condensation on finned horizontal tubing has yet to be performed, however, without making significant simplifications.

All of the results above are based on the Gregorig premise that surface forces act to thin the condensate film on the convex portions of the fins (where heat transfer is high) and to thicken the film in the troughs (where heat transfer is low). In marked contrast to this model is the scheme proposed by Thomas [114] for a vertical tube that has circular or rectangular fins to draw condensate away from the tube surface into the fillets, thereby thinning the film *between the fins*. This technique does not rely on conduction through the fins, and is effective even when loosely fitting wires are used. Even though this work was done for vertical surfaces, the same principle may be applied to horizontal tubes. For example, some recent data for ammonia condensing on the outside of horizontal, wire-wrapped tubes (about four wraps per inch) gave external heat transfer coefficients about three times the Nusselt value for smooth tubes [115]. Film condensation data with horizontal commercially available corrugated tubes have shown enhancements as large as 70% [116–120].

Heat transfer enhancement has also occurred when condensate film drainage from a horizontal tube is modified. Glicksman et al. [121] interrupted the condensate film on copper tubing by using Teflon tape, 3.2 mm wide and 0.15 mm thick, placed at certain positions along the tube. They found, however, that the best position for the tape was along the bottom of the tube, and this location gave an average heat transfer coefficient 1.6 times the smooth-tube value with no tape. Desmond and Karlekar [122] tested a stainless steel tube that had a 9.1-mm-wide by 0.025-mm-thick film of Emralon, a nonwetting fluoroplastic, attached at the bottom. They pointed out that this location of the tape gave the greatest incremental increase in heat transfer, which amounted to a 20% increase in the overall heat transfer coefficient. Condensate retention of horizontal integral-fin tubing was recently reported on by Rudy and Webb [123]. They performed a series of experiments to measure static liquid retention in integral-fin tubing having variable fin densities, and showed that surface tension forces have a significant effect on film drainage.

Most of the enhanced heat transfer results obtained to date are for single horizontal tubes, and few data are available for tube bundles where both condensate inundation and vapor shear are important. With dropwise conditions, there are data which show that condensate falling on a horizontal tube may not deteriorate the heat transfer coefficient as shown earlier for film condensation, and in certain circumstances condensate inundation may actually increase the heat transfer coefficient [56, 59, 64]. Data obtained during filmwise condensation on a horizontal, helically wire-wrapped, smooth tube show a similar trend [124]. There is also evidence that during film condensation on corrugated tubing, the effect of condensate inundation is not as pronounced as for smooth tubes

[116, 119]. The inundation trends mentioned above were obtained with low-velocity steam in a gravity-dominated regime. The exact behavior of these surfaces with high-velocity steam moving in various directions within a tube bundle remains to be determined, and will require careful research methods to elucidate the complex mechanisms that are occurring.

SHELL-SIDE PRESSURE DROP

Despite the importance of knowing the shell-side pressure loss in condenser design, little research has been performed on shell-side, two-phase flow with condensation. Most of the aforementioned shell-side heat transfer research does not include pressure drop measurements, in part because of the great difficulty in obtaining accurate pressure data during condensation. As a result, the pressure drop information available in the literature pertains almost entirely to adiabatic flow.

For simplicity, shell-side losses in general may be calculated by using single-phase (i.e., dry-tube) correlations of the form [10]:

$$\Delta P = 4 f_m N_t \rho \frac{U_m^2}{2} \tag{34}$$

where N_t = number of tube rows
U_m = average maximum velocity in the bundle (i.e., based on minimum flow area)
f_m = friction factor, which depends on U_m

Single-phase friction factors in tube bundles may be obtained from a variety of sources [125], and for a limited Reynolds number range may be expressed simply as [126]:

$$f = \frac{a}{\mathrm{Re}^n} \tag{35}$$

where n is the Blasius exponent, which in general is near 0.2, and the coefficient a depends on the tube bank geometry (i.e., staggered or in-line, and s/d). Davidson and Rowe [10] have shown that the above technique successfully predicts pressure losses during horizontal two-phase flow in a condensing bank. Brickell [71], however, points out that significant differences occur with either upflow or downflow, and suggests that the differences are due to an additional two-phase gravitational term that exists when a significant amount of condensate holdup occurs within the bundle. Figure 15 shows some unpublished air-water friction factor data from Oak Ridge National Laboratory [127], which exhibit the above-mentioned difference with upflow or downflow. With little or no water flow, the data are close together, as indicated by curves 1, 2, 3, and 5. At high water rates, however, the data for both downflow (curve 4) and upflow (curve 6) are substantially higher than in the dry-tube case (e.g., at $\mathrm{Re} \simeq 10^3$, f increases by $\simeq 60\%$), and the deviation appears to get worse at lower Reynolds numbers. The influence of large amounts of condensate, in the form of thick, wavy films attached to the tubes and large droplets entrained within the flow, may therefore be significant and should be properly accounted for in modeling shell-side losses.

In addition to the usual losses experienced by the vapor due to contractions and expansions at the inlet and exit of the condenser tube bundle, a sizable pressure drop can occur due to friction and momentum effects encountered in flowing through the tube bundle itself [128]. Unfortunately, it is difficult to calculate this tube bundle pressure drop due to the complexities that occur with phase change. Lee et al. [129] suggested that the occurrence of condensation influences the vapor pressure drop in two ways. First, the suction effect caused by the mass transfer of the condensing vapor reduces the momentum flow in the flow direction, increases the shear stress on the tube, and delays the separation point. Second, there are two-phase effects due to the formation of the liquid film on the tube and entrainment of this liquid into the vapor space. The influence of suction on the shear stress and the separation point was measured by Aly and Cunningham [130] with air flowing over a specially instrumented, porous cylinder that could be located in any position

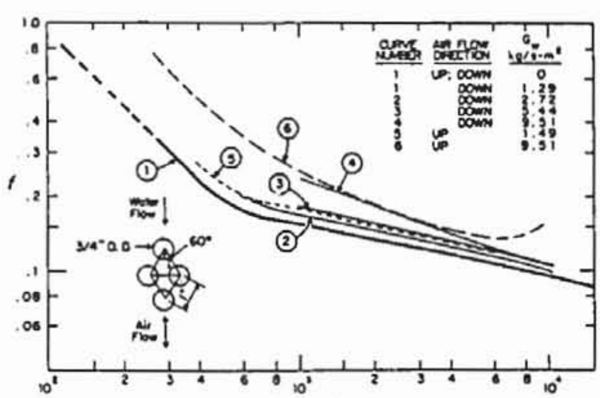

Figure 15 Effect of two-phase flow on friction factor [127].

within a staggered tube bundle seven rows deep. Figure 16 shows their data for the first row of tubes at a Reynolds number of 60,000. It is evident that as the suction velocity V_0 increases, the shear stress increases significantly in magnitude and the separation point is delayed to about 110°. They point out, however, that while this dramatic increase in shear stress occurs, the contribution of the pressure drag to the total drag does not change appreciably with suction.

Another complicating feature of vapor flow with condensation is that the mass extraction (simulated by suction in the investigations mentioned above) causes the vapor velocity to change throughout the bundle, making it difficult to use an expression similar to Eq. (34). As pointed out earlier in Table 1, depending on the operating pressure level of the condenser, the vapor velocity may increase or decrease as the vapor traverses the tube rows. If the velocity decreases, a pressure recovery may actually occur, leading to smaller losses. Lee et al. [129] measured the pressure losses in both an in-line and a staggered bundle, with a tight spacing of tubes ($s/d = 1.25$), during simulation of condensation by using porous tubes with suction. Their suction range was substantially larger than that of Aly and Cunningham [130] with $0 < (V_0/U_a)\sqrt{\mathrm{Re}} < 5$. They pointed out that their pressure readings fluctuated substantially, leading to considerable scatter, and were very sensitive to the precise location of their pressure taps. Their results confirmed the effect that suction produces a substantial reduction in the pressure drop, with most of the reduction occurring in the first few rows of tubes. Their data showed that the pressure drop for tube banks with suction can be predicted reasonably well from nonsuction pressure coefficients provided a mean dynamic pressure is used as defined below:

$$\tfrac{1}{2}\rho_m \bar{U}_m^2 = \tfrac{1}{2}\rho_m\left[\tfrac{1}{2}(U_{m,i}^2 + U_{m,e}^2)\right] \tag{36}$$

Nicol et al. [131] obtained some recent experimental data for condensation rates and pressure drops during cross flow of steam in a small tube bundle with widely spaced tubes (s/d near 1.7). Data were taken with both an in-line and a staggered geometry, and their value for the drag coefficient is plotted against steam Reynolds number in Fig. 17. For both the in-line and staggered geometries, the drag coefficient with condensation is substantially less than the dry-tube value. This decrease is attributed to the delay in the onset of separation caused by the condensation process. The authors pointed out that their data were lower than those of Fujii et al. [62], presumably due to the fact that the pressure levels were an order of magnitude different. They condensed at pressures from 0.2 to 0.8 bar, while Fujii et al. [62] condensed at pressures from 0.01 to 0.07 bar.

Various methods have been proposed to predict the two-phase frictional pressure drop. Diehl [132] obtained adiabatic two-phase flow data for downflow in both staggered and in-line tube banks. He showed that the data for $\Delta P_{2\phi}/\Delta P_{GO}$ were correlated empirically with the following type of functional relationship:

$$\frac{\Delta P_{2\phi}}{\Delta P_{GO}} = f\left[\frac{\mathrm{LVF}}{(\rho_G/\rho_L)(\mathrm{Re}_{GO})^n}\right] \tag{37}$$

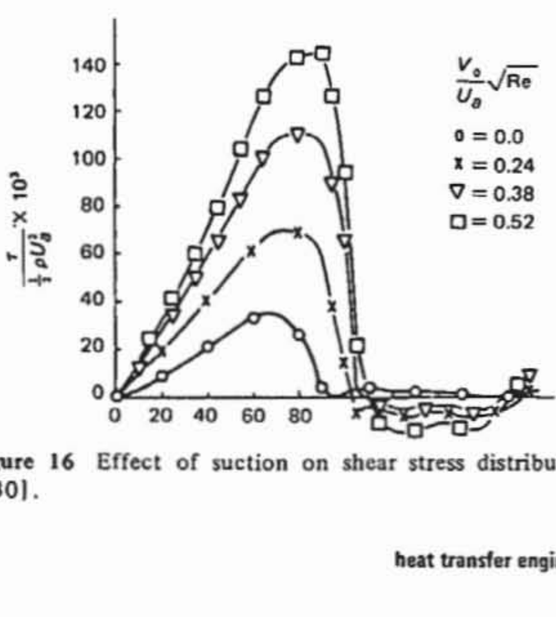

Figure 16 Effect of suction on shear stress distribution [130].

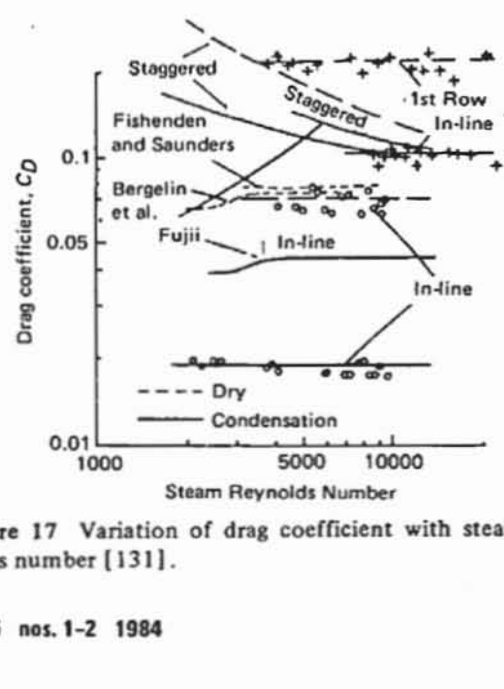

Figure 17 Variation of drag coefficient with steam Reynolds number [131].

where LVF = superficial liquid volume fraction based on a homogeneous flow model
n = 0.5 for staggered tubes and 0.2 for an in-line arrangement

No attempt was made, however, to provide an analytical expression for the function f. Collier [133] compared the experimental data of Diehl and Unruh [134] for gas-liquid mixtures in horizontal cross flow with the homogeneous flow model of Wallis [135]. This comparison is shown in Fig. 18, where $\phi_{GO}^2 = (dP_F/dz)/(dP_F/dz)_{GO}$ is plotted against ξ [equal to $(1-\beta)v_g/v_f$]. It is readily apparent that the data are in satisfactory agreement with the very simple homogeneous flow relationship:

$$\phi_{GO}^2 \simeq \left(\frac{1}{1+\xi}\right) \tag{38}$$

Grant and Chisholm [136, 137] conducted tests with air-water mixtures in cross flow in two tube banks having 39 and 165 tubes, respectively. They observed various flow patterns depending on the liquid and gas flow rates, and developed an improved calculational procedure to predict the two-phase pressure drop that depends on the type of flow occurring within the tube bundle [138]. The mapping of two-phase flow regimes during condensation has received considerable attention in recent years [139–143], and Fig. 19 shows one type of flow regime map giving the pertinent parameters and flow patterns during shell-side conditions, and compares them to the Baker map for tube-side conditions [140]. Notice that the gravity-dominated regimes (stratified, stratified-spray, and slug) and the shear-dominated regimes (spray and annular) appear to fall in the same regions when the data are plotted with the modified Baker parameters B_v and B_l. These parameters,

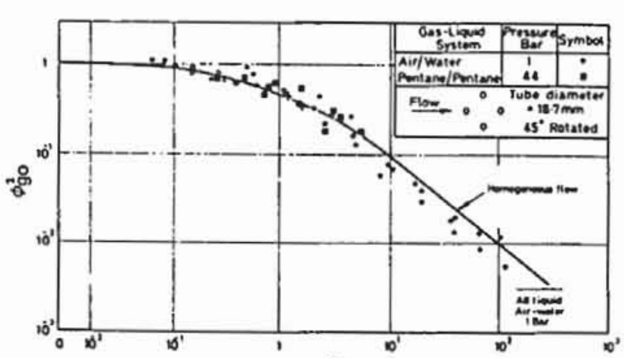

Figure 18 Comparison of Diehl and Unruh [134] two-phase pressure drop data with homogeneous flow model [133].

however, are empirically derived, and there is recent evidence that more general parameters may be found [142, 143].

Grant and Chisholm [136] recommended the following expression, which correlated their data:

$$\phi_{LO}^2 = \frac{dp_F/dz}{(dp_F/dz)_{LO}}$$
$$= 1 + (\Gamma^2 - 1)[Bx^{(2-n)/2}(1-x)^{(2-n)/2} + x^{2-n} \tag{39}$$

where n = Blasius exponent in the friction factor expression, Eq. (35)
x = mass flow quality
$\Gamma^2 = \Delta P_{GO}/\Delta P_{LO} = f_{GO}\rho_L/f_{LO}\rho_G$

With n equal to 0.46, the coefficient B, which varies with flow regime, was determined to be 0.75 for spray and bubbly flow, and 0.25 for stratified and stratified-spray flow [136]. An improved, more general procedure was more recently proposed [138].

Ishihara et al. [144] recently provided a comprehensive critical review of the existing two-phase frictional pressure drop correlations for flow across tube banks. They examined the available published data, compared them with existing correlations, and found that no published correlation is general enough to be used reliably to predict all the data. They then reexamined the Martinelli separated flow approach, which assumes that both the liquid and vapor phases experience the same pressure drop but do not have the same velocity. They tried various forms of pressure drop correlations as a function of the Martinelli parameter X_{tt}, given by Eq. (29), and proposed the following general forms:

$$\phi_{LO}^2 = \frac{\Delta P_{2\phi}}{\Delta P_{LO}} = 1 + \frac{C}{X_{tt}} + \frac{1}{X_{tt}^2} \tag{40}$$

for $Re_L > 2000$, and

$$\phi_{GO}^2 = \frac{\Delta P_{2\phi}}{\Delta P_{GO}} = 1 + CX_{tt} + X_{tt}^2 \tag{41}$$

for $Re_L \leqslant 2000$. They pointed out that C is an empirical adjustment factor, which in general is a function of the pertinent two-phase flow variables:

$$C = f\left(X_{tt}, \eta, \frac{1-x}{x}\right) \tag{42}$$

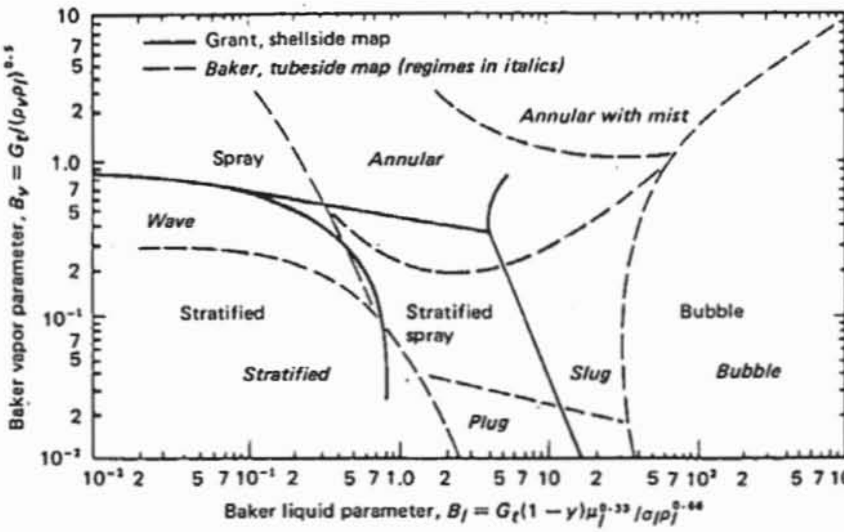

Figure 19 Adaptation of Baker flow map to horizontal shell-side two-phase flow [144].

The variable η is proportional to the ratio of the vapor shear force to the gravity force, and $(1-x)/x$ is the ratio of liquid to vapor present, so it would be reasonable that the factor C would depend on the particular flow regime in question. Ishihara et al. [144] did not present a final functional form for C, but they showed that, by using a constant value of $C = 8.0$ in Eq. (40), good results could be obtained in correlating the data, as shown in Fig. 20, especially for small values of X_{tt} (i.e., high vapor fraction). They also recommended that, since most of the data have been obtained with small bundles, it is most important to obtain data for large tube bundles, which are more representative of operating condensers.

COMPUTER MODELING

As pointed out earlier, the standards in use today to design condensers fail to take into account shell-side conditions [13, 14]. They neglect the problems associated with noncondensable gases, and do not consider the size and shape of the shell or the details of the tube bundle layout. As a consequence, all of the benefits to be derived from the abovementioned developments in shell-side heat transfer and two-phase flow (such as the design of new tube bundle arrangements, or the diagnostic analyses of poorly operating condensers) must depend on numerical modeling techniques with large digital computers. The need for such techniques in heat exchanger design has long been known, but because of the complexities and costs involved, their development and use in industry have been slow [10, 145–147].

Early efforts to model the thermal performance of condensers were limited essentially to one-dimensional routines in the plane perpendicular to the tubes [148–151]. Barsness [148] divided the longitudinal length of the condenser into a number of short bays. For each bay, he considered radial flow through a condenser tube bank that was bounded on the outside by the steam distribution lane and on the inside by the air vent. He assumed that a zone, containing a large number of con-

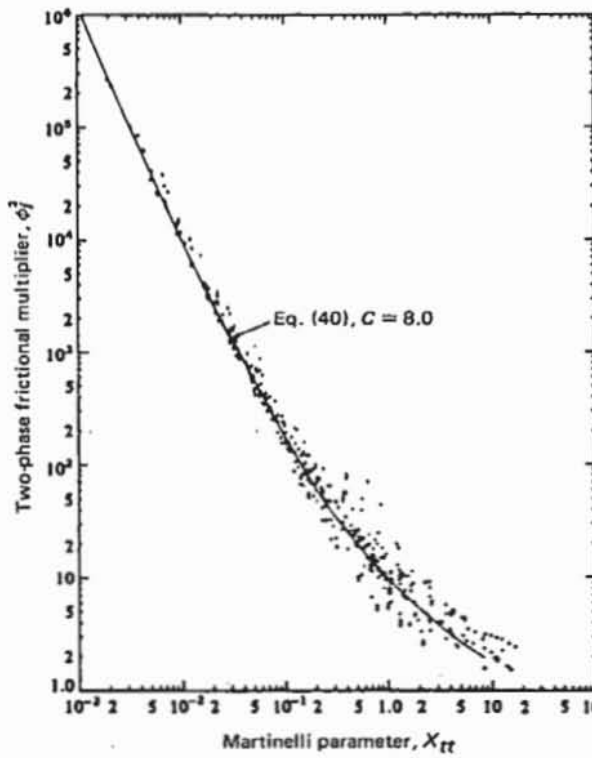

Figure 20 Correlation of shell-side pressure drop data using the Martinelli parameter [144].

denser tubes of short length, can be represented by a smaller number of tubes having average properties and average heat transfer expressions. A number of these zones were joined together to make up the entire flow field. For a given zone, once the steam entered from the outside, it was restricted from flowing across the side boundaries to another zone. Also, the steam was assumed to flow with no axial component. Two-phase pressure drop calculations were made by the method of Diehl and Unruh [134]. For a given zone, the average overall heat transfer coefficient was calculated by summing up the individual resistances. Overall condenser performance was obtained by integrating over all the zones within a given bay and then from bay to bay along the entire length of the condenser. A large number of calculations were made, requiring the use of a digital computer. Both laboratory tests and field test data were utilized to verify the predictions of the code, and good agreement was obtained. A similar type of radial flow code, called ORCON 1, was developed at Oak Ridge National Laboratory to model the flow in circular bundles [149].

Emerson [150] developed a one-dimensional code to model the downflow of steam through a horizontal bundle of tubes. He assumed that the velocity distribution is uniform at any horizontal section. He computed an overall coefficient at each row of tubes, using separate resistances due to the water-side coefficient, fouling, tube wall, noncondensable gases, and condensate film. He found that when he compared his predictions with data obtained from a small experimental condenser, as shown in Fig. 21, the one-dimensional model was not able to accurately predict the steam flow along the bypass lane on the left side of the bundle. He therefore proposed a two-dimensional model to allow the steam to flow in any direction in the plane perpendicular to the tubes, and derived the equations to calculate the distribution of steam velocity, pressure, and air concentration within the tube bundle. Concern was expressed regarding convergence of the code, however, due to the nonlinear character of the equations. Wilson [151] developed an iterative technique to solve a large number of nonlinear equations. He postulated an imaginary mesh over the tube bank such that each mesh line represented the steam path between two tubes and each node point represented a branching point for the steam. The resulting mesh for a tube bundle having an equilateral pitch would be hexagonal, and each tube would have six separate heat flux terms calculated by summing the various thermal resistances in series. He utilized an expression for noncondensing gas flow over tube banks [126] in order to calculate the pressure drop between each pair of nodes. To solve his nodal equations, he assumed a pressure distribution and examined the mass balance at each node. The pressure distribution was iterated by Newton's method until the residuals from the nodal mass balances reduced to zero. Using this technique with a Univac 1108 computer, it required about 10 min of computation time to obtain a solution for a condenser with 1000 tubes. He compared his predicted results with data from an experimental condenser having 218 tubes and found excellent agreement. He was also able to use his computer code to analyze the flow within the lower bundle of a two-pass large power station condenser to suggest modifications for improved performance.

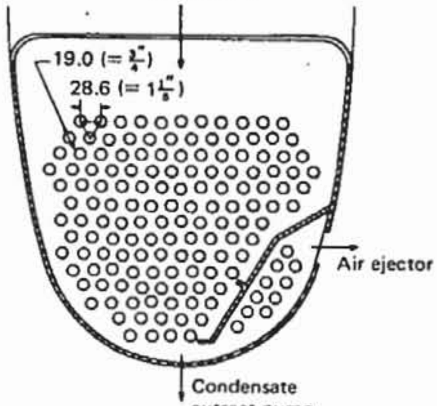

Figure 21 Cross section of NEL test condenser [154].

The model of Wilson [151], however, does not include steam inertia effects, and since the mesh is uniform and very fine, all parts of the condenser are treated equally and the solution for large condensers may take a significant amount of computer time. Furthermore, the code calls for specification of the local conditions for each tube within the bundle, and in light of the current understanding of the complex nature of shell-side conditions, the specification of such fine detail is perhaps unwarranted.

As an alternative, a continuum approach was taken by Davidson [10, 152], where the steam was considered to be flowing in an anisotropic porous medium that allows for nonuniform blockage effects of the tubes and the removal of steam due to condensation. Again, the flow was assumed to be two-dimensional in a plane perpendicular to the cooling water flow direction. As shown in Fig. 22, two distinct but interrelated regions were treated: the untubed areas, where viscous effects were small, and the tube bundle areas, where the flow was influenced by the resistance of the tubes and by the condensation of steam and the resulting production of condensate. Assuming a rectangular coordinate system, the equations of motion were expressed as [10]:

$$F_x = \frac{\partial P}{\partial x} + \frac{\partial}{\partial x}(\rho u^2) + \frac{\partial}{\partial y}(\rho uv) \tag{43}$$

$$F_y = \frac{\partial P}{\partial y} + \frac{\partial}{\partial x}(\rho uv) + \frac{\partial}{\partial y}(\rho v^2) \tag{44}$$

The distributed forces per unit volume included a flow resistance term and a condensation rate term:

$$F_x = -K\rho uq - uQ \tag{45}$$

$$F_y = -K\rho vq - vQ \tag{46}$$

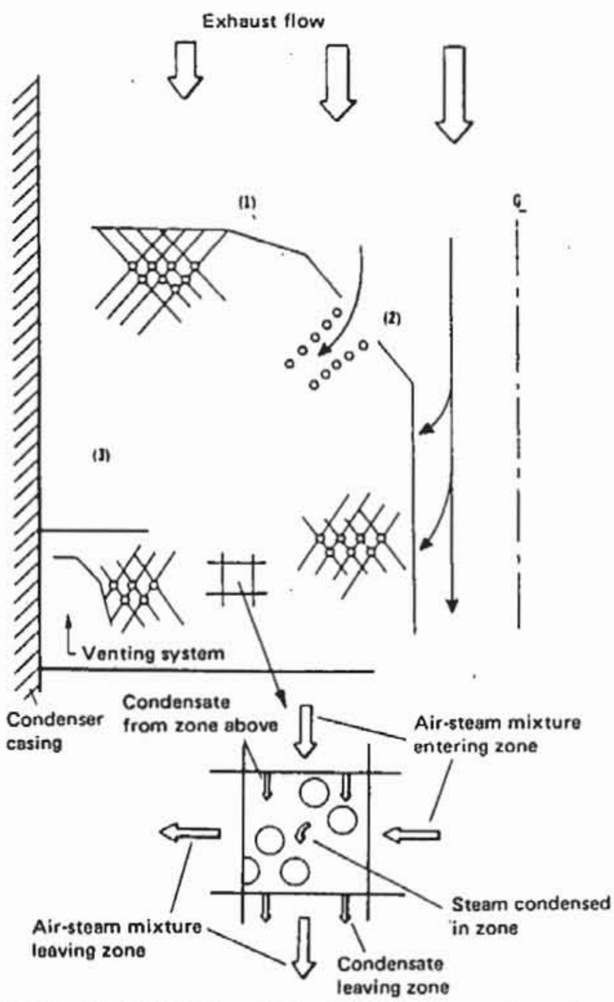

Figure 22 Condenser flow regions in two-dimensional computer model [10].

where K is a friction factor, ρ is the density of the steam-gas mixture, Q is the local condensation rate per unit volume (calculated from a local overall heat transfer coefficient), and q is the local velocity, $\sqrt{u^2 + v^2}$. The equation of continuity for the mixture was:

$$\frac{\partial}{\partial x}(\rho u) + \frac{\partial}{\partial y}(\rho v) = -Q \tag{47}$$

The conservation equation for noncondensable gases was also provided as [10]:

$$\nabla \cdot (\rho \phi \mathbf{u}) + (j_s - j_a) = \nabla \cdot (D\rho \nabla \Pi) + \nabla \cdot [D\rho(\Pi - \phi)\nabla \ln P] \tag{48}$$

where D is a diffusion coefficient, j_s and j_a are mass removal rates per unit area for steam and noncondensables, respectively, and

$$\phi = \frac{\rho_s - \rho_a}{\rho}$$

$$\Pi = \frac{P_s - P_a}{P}$$

The differential equations above are coupled and must therefore be solved simultaneously. Butterworth [153] examined the combined form of Eqs. (43)–(47) and discussed the details of tube resistance, anisotropy in tube bundles, the addition of viscous terms due to velocity gradients across the tube bundle, axial flow effects, and corrections to the inertial terms. He concluded that modeling the flow in tube bundles as flow in an anisotropic porous media is an extremely powerful technique in relatively early stages of development, and there is a vital need for both theoretical and experimental research to extend the technique.

Davidson and Rowe [10] used the equations above to model the conditions in operating condensers in the United Kingdom. They discretized the flow field, using a finite-difference technique, and solved the resulting algebraic equations with a modified implicit iterative procedure found to be very stable. Figure 23 shows the resulting pressure contours for the multifolded condenser tube bundle shown earlier in Fig. 4*b*. A moderate pressure drop of only 2 mbar exists between the top of the bundle and the air removal section in the lower left-hand portion of the bundle. Notice that the radial steam lanes allow the steam to

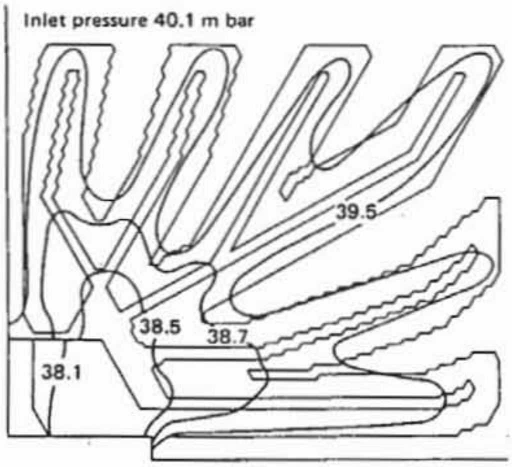

Figure 23 Calculated pressure contours from two-dimensional computer code [10].

penetrate into the tube bundle with little pressure loss. In some designs, however, the steam lanes may be narrow, leading to high vapor velocities and significant pressure losses. In these cases, it is very important to be able to model the flow in the lanes accurately by using two-dimensional considerations.

More recently, Shida et al. [154] pointed out that the technique of Davidson and Rowe [10] was restricted to condensers with simple shapes because of their assumed rectangular mesh pattern and finite-difference technique. Shida et al. therefore proposed a modified FLIC (fluid in cell) method [155], which uses a triangular mesh pattern conventionally used in the finite-element method. They performed calculations by an upwind, two-step Lagrangian and Eulerian time-marching technique and compared their results against experimental data for two types of test condensers. Figure 24*a* shows their triangular mesh pattern for the NEL test condenser shown earlier in Fig. 21. The hatched lines designate the boundaries of the tube bundle and the air cooler section. Figure 24*b* shows their calculated flow pattern for this condenser where the velocity vectors (the arrows) in the tube bundle correspond to the mean velocity of maximum flow area. Notice that part of the steam on the left side of the bundle flows down the access lane directly to the air cooler section without ever penetrating the bundle. They showed that by putting a horizontal baffle plate in this access lane about two-thirds of the way up the bundle, steam can be diverted into the bundle, increasing the condensation rate by 7%.

Marto and Nunn [156] used a modified version of the one-dimensional code ORCON 1 [149] to study the use of heat transfer enhancement to improve steam condenser performance. Figure 25 shows a schematic drawing of the circular geometry they analyzed. They assumed that the steam flow was symmetrical about the vertical centerline. It was distributed around the circumference in such a way that there was no circumferential pressure gradient at the condenser outlet (the concentric air cooler section in the center of the bundle). The tube field was divided into six pie-shaped sectors of 30° each. For a given sector, at any radial position or tube row, an average overall heat transfer coefficient was calculated for the tubes in that particular row of the sector, using the thermal resistances in series. The code ORCON 1 has the simple capability of inserting heat transfer

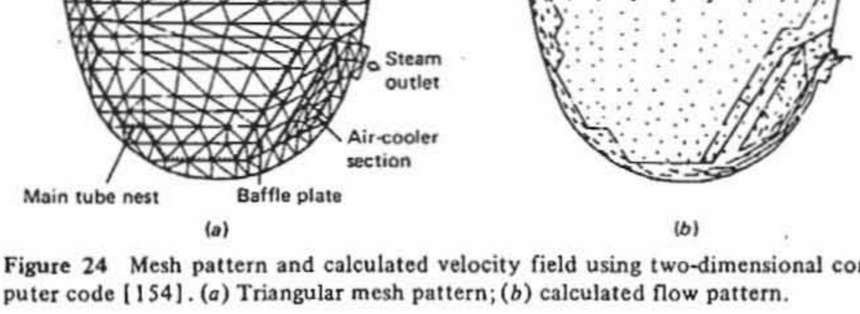

Figure 24 Mesh pattern and calculated velocity field using two-dimensional computer code [154]. (*a*) Triangular mesh pattern; (*b*) calculated flow pattern.

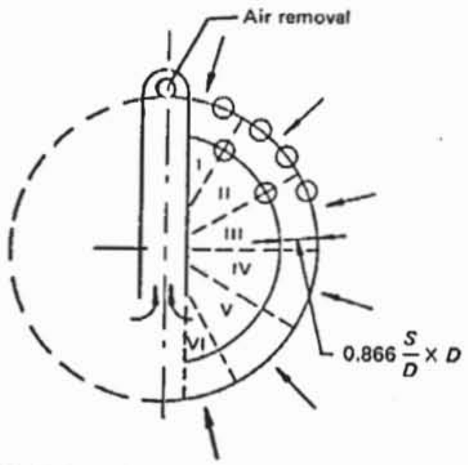

Figure 25 Schematic representation of ORCON 1 tube bundle layout [156].

enhancement factors E_i and E_o as multipliers of the calculated heat transfer coefficients on the tube-side and shell-side, respectively. The effect of this enhancement on a baseline condenser having 1646 smooth copper-nickel tubes in half of the bundle was examined. Figure 26 illustrates the effect of internal and external enhancement in terms of the length of tubes necessary to maintain the baseline heat duty for the same cooling water velocity (a pumping power increase was allowed). The results show, for example, that a tube-side enhancement of 2.0 and a shell-side enhancement of 1.5 (as available with some commercial condenser tubing) could lead to a condenser length reduction of 25%. They pointed out that in utilizing enhanced heat transfer techniques in large condenser tube bundles, care must be exercised in balancing the thermal resistances. Apparently, different regions of the condenser may be limited

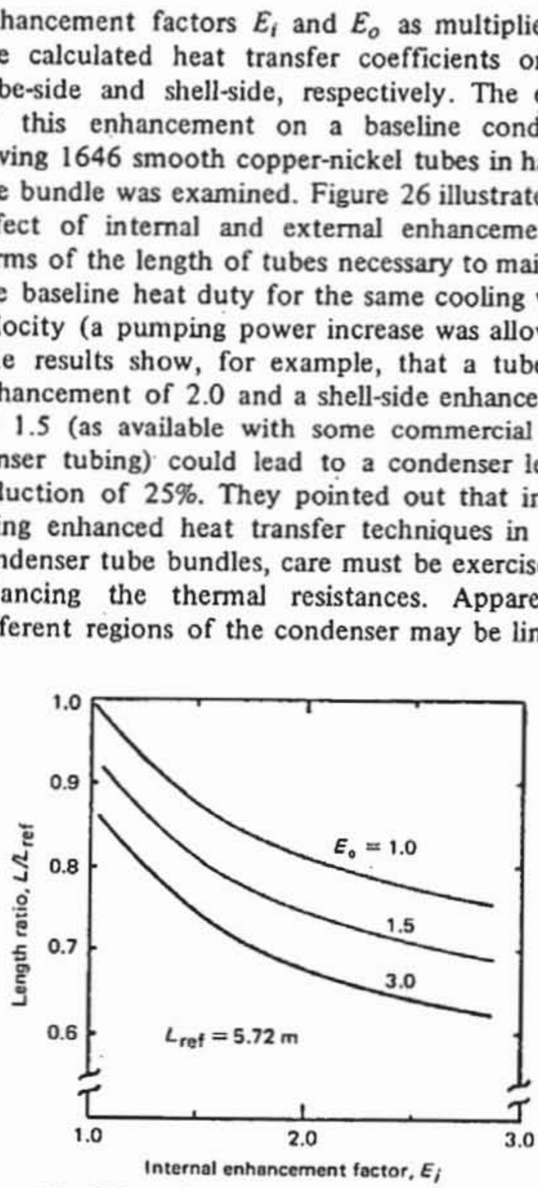

Figure 26 Effect of internal and external enhancement on condenser tube length [156].

by the tube-side or shell-side resistance. If this is the case, a hybrid enhanced heat transfer design may be contemplated, using numerical optimization techniques [157].

CONCLUSIONS

In recent years, considerable research has been conducted to aid in understanding the fluid flow and heat transfer processes that occur during shell-side condensation. In addition, the advent of large-capacity, efficient digital computers has made it feasible to model these phenomena with reasonable success.

It appears, however, that there is still a critical shortage of thermal/hydraulic data for large tube bundles, making it difficult to verify analysis routines. In the future, therefore, large-bundle tests must be carried out under carefully controlled experimental conditions and with sufficient instrumentation to measure the pressure drop and heat transfer for various vapor flow velocities and directions, and over a range of heat fluxes. Particular attention should be given to obtaining data at very high vapor velocities and small heat fluxes, for which no data exist at present. In this way, additional insight may be gained into combined vapor shear and condensate inundation, and the important influence of condensate holdup and/or entrainment on thermal/hydraulic performance may be ascertained. Such tests should, of course, be repeated with various heat transfer enhancement techniques and with varying amounts of noncondensable gases.

Additional efforts should be made to interpret and analyze data in terms of flow regimes and two-phase forced convection. The modeling of shell-side condensation as flow in anisotropic, porous media deserves more attention in the years ahead, as well as the development of improved numerical techniques to enable large tube bundles to be analyzed in a small amount of computer time. Numerical optimization techniques may be especially useful in such preliminary design studies.

It is important to realize, however, that the research progress referred to above must eventually find its way into the hands of condenser designers and manufacturers. As Mayhew [158] has put it: "Theory, if it cannot provide an accurate design tool, can at least show how to progress from one design to a better one." Of course, the degree of sophistication of new computer codes and improved designs will depend ultimately on the economics behind the need for advanced condensers of the future.

NOMENCLATURE

A	surface area
B	Baker parameter (Fig. 19)
B	coefficient [Eq. (39)]
C	coefficient [Eq. (1)]
C	empirical adjustment factor [Eqs. (40) and (41)]
C_D	drag coefficient
C_f	friction coefficient
C_n	correction factor for inundation due to n tubes
c_p	specific heat
C_v	correction factor for vapor shear
D	diffusion coefficient
d	tube diameter
F	dimensionless quantity [Eq. (10)]
F_x	body force per unit volume in x direction
F_y	body force per unit volume in y direction
F_1	Heat Exchange Institute (HEI) correction factor for fouling
F_2	HEI correction factor for tube wall resistance
F_3	HEI correction factor for cooling water inlet temperature
f	friction factor
Fr	Froude number $(= U_\infty^2/gd_o)$
G	mass flow rate per unit area
G	dimensionless quantity [Eq. (13b)]
g	acceleration due to gravity
G_n	flow rate of condensate per unit area forming on nth tube
$(\Sigma G)_n$	total flow rate of condensate per unit area running off nth tube
Ga	Galileo number $(= d_o^3 g/\nu_L^2)$
H	phase change number $[= c_p(T_s - T_w)/h_{fg}]$
h	heat transfer coefficient
$\bar{h}$	average heat transfer coefficient
$\bar{h}_n$	average heat transfer coefficient for a vertical row of n tubes
h_{fg}	latent heat of vaporization
K	flow resistance factor
k	thermal conductivity
j	mass flow rate per unit area
LMTD	log mean temperature difference
$\dot{m}$	mass flow rate
N_t	number of tube rows
n	number of tubes in a vertical row
Nu	Nusselt number $(= hd_o/k_L)$
P	pressure
ΔP	pressure drop
Pr	Prandtl number $(= \mu c_p/k)$
Q	local condensation rate per unit volume
q	local steam velocity $(= \sqrt{u^2 + v^2})$
R	thermal resistance
Re	Reynolds number
$\mathrm{Re}_{2\phi}$	two-phase Reynolds number $(= U_\infty d_o/\nu_L)$
s	inundation exponent [Eq. (23)]
Sc	Schmidt number $(= \nu/D)$
T	temperature
ΔT_s	drop in saturation temperature
U	overall heat transfer coefficient
U	vapor velocity
$\bar{U}$	average vapor velocity
u	condensate velocity
$\mathbf{u}$	fluid velocity
u	vapor velocity in x direction
v	cooling water velocity
v	vapor velocity in y direction
V_o	suction velocity at the tube wall surface
w	weight fraction of noncondensable gas
X	dimensionless quantity [Eq. (13a)]
x	vapor quality
X_{tt}	Lockhart-Martinelli parameter [Eq. (29)]
Y	local inundation value $[= (\Sigma G)_n/G_n]$
z	distance along flow direction
β	vapor volumetric quality
ξ	dimensionless quantity $[= (1-\beta)v_g/v_f]$
μ	dynamic viscosity
ν	kinematic viscosity
π	$(P_s - P_a)/P$
ϕ	$(\rho_s - \rho_a)/\rho$
ρ	density
τ	shear stress
ζ	dimensionless quantity [Eq. (15)]

Subscripts

a	air
c	condensate
e	exit
f	fouling; liquid
F	friction
G, g	gas
GO	gas only
gr	gravity-controlled
i	inlet; inside; interface
L, l	liquid
LO	liquid only
m	mixture; maximum
n	nth row

N	Nusselt
nc	noncondensable
o	outside
s	saturation; steam
sh	shear-controlled
v	vapor
w	wall; water
x	x direction
y	y direction
Y	local inundation value
ϕ	potential flow
2ϕ	two-phase
1	first row
∞	free-stream

REFERENCES

[1] Silver, R. S., Some Aspects of the Development of the Condenser from the Time of James Watt, *Symposium to Commemorate the Bicentenary of Watt's Patent*, pp. 27–90, Univ. of Glasgow, U.K., September 1969.

[2] Sebald, J. F., A History of Steam Surface Condensers for the Electric Utility Industry, *Heat Transfer Eng.*, vol. 1, no. 3, pp. 80–87, 1980.

[3] Robertson, R. C., Waste Heat Rejection from Geothermal Power Stations, ORNL/TM-6533, December, Oak Ridge National Laboratory, Oak Ridge, Tenn., 1978.

[4] Sebald, J. F., Main and Auxiliary Condensers, *Marine Engineering*, pp. 450–453, Society of Naval Architects and Marine Engineers, New York, 1971.

[5] Silver, R. S., An Approach to a General Theory of Surface Condensers, *Proc. Inst. Mech. Eng.*, vol. 178, pt. 1, no. 14, pp. 339–357, 1963–1964.

[6] Editors of *Power magazine*, Power-Generation Systems, p. 93, McGraw-Hill, New York, 1967.

[7] Shklover, G. G., Rosinskiy, A. Z., Buyevich, A. V., and Larvov, Y. I., Condensers for Steam Turbines, *Heat Transfer–Sov. Res.*, vol. 13, no. 2, pp. 65–77, 1981.

[8] Chatel, F. J., Steam Condenser Practice and Performance, *Mech. Eng.*, vol. 49, no. 3, pp. 227–242, 1927.

[9] Emerson, W. H., Steam Turbine Condensers, NEL Rept. 619, pp. 1–10, National Engineering Laboratory, East Kilbride, Scotland, August 1976.

[10] Davidson, B. J. and Rowe, M., Simulation of Power Plant Condenser Performance by Computational Methods: An Overview, in *Power Condenser Heat Transfer Technology*, eds. P. J. Marto and R. H. Nunn, pp. 17–49, Hemisphere, New York, 1981.

[11] Gotoda, H. and Izumi, S., A Modern Condenser Design, *Proc. Inst. Mar. Eng.*, pp. 253–273, March 1977.

[12] Wilson, J. L., NEL Two-dimensional Condenser Computer Program, NEL Rept. 619, pp. 132–150, National Engineering Laboratory, East Kilbride, Scotland, August 1976.

[13] Heat Exchange Institute, *Standards for Steam Surface Condensers*, 7th ed., New York, 1978.

[14] British Electrical and Allied Manufacturers' Association, *Recommended Practice for the Design of Surface Type Steam Condensing Plant*, London, 1967.

[15] Orrok, G. A., The Transmission of Heat in Surface Condensation, *Trans. ASME*, vol. 32, pp. 1139–1214, 1910.

[16] Wenzel, L. A., in *Power Condenser Heat Transfer Technology*, eds. P. J. Marto and R. H. Nunn, pp. 182–183, Hemisphere, New York, 1981.

[17] Macnair, E., Introduction, in *Power Condenser Heat Transfer Technology*, eds. P. J. Marto and R. H. Nunn, p. 5, Hemisphere, New York, 1981.

[18] Taborek, J., in *Power Condenser Heat-Transfer Technology*, eds. P. J. Marto and R. H. Nunn, pp. 425–426, Hemisphere, New York, 1981.

[19] Campbell, I., Hall, K., and Searle, N. K., The Use of Titanium in Seawater Heat Exchangers, *Cooling With Sea Water*, p. 124, Institution of Mechanical Engineers, London, 1979.

[20] Rowe, M., Notes on Steam Condensers, private communication, June 1979.

[21] Steam Plant Surface Condenser Leakage Study, EPRI NP-481, vols. 1 and 2, Bechtel Corp., San Francisco, Calif., March 1977.

[22] Chenoweth, J. M., Flow-induced Tube Vibrations in Shell-and-Tube Heat Exchangers, ERDA Rept. SAN/1273-1, Heat Transfer Research Incorporated, Alhambra, Calif., February 1977.

[23] Nusselt, W., Die Oberflachen-Kondensation des Wasserdampfes, *VDI Z.*, vol. 60, pp. 541–546 and 569–575, 1916.

[24] Taborek, J., Design Methods for Heat Transfer Equipment–Critical Survey of the State of the Art, in *Heat Exchangers: Design and Theory Sourcebook*, eds. N. Afgan and E. U. Schlünder, pp. 59–69, Hemisphere, New York, 1974.

[25] Davidson, B. J. and Preston, S. B., Heat and Mass Transfer in Condensers, *UK/USSR Symposium 1976*, pp. 1–18, Rept. No. 5, Central Electricity Research Laboratories, Leatherhead, U.K., May 1976.

[26] Butterworth, D., Developments in the Design of Shell-and-Tube Condensers, ASME paper 77-WA/HT-24, Atlanta, Ga., December 1977.

[27] Semeria, R. and Hewitt, G. F., Aspects of Heat Transfer in Two-Phase Gas-Liquid Flow, in *Heat Exchangers: Design and Theory Sourcebook*, eds. N. Afgan and E. U. Schlünder, pp. 344–351, Hemisphere, New York, 1974.

[28] Butterworth, D., Film Condensation of Pure Vapor, in *Heat Exchanger Design Handbook*, vol. 2, pp. 2.6.2-9 to 2.6.2-12, Hemisphere, New York, 1982.

[29] Kutateladze, S. S., *Heat Transfer in Condensation and Boiling*, Mashgiz, Moscow, 1952.

[30] Fuks, S. N., Condensation of a Vapor Flow Over a Horizontal Tube, *Izvestiya Vses. Teplotekh. Inst.*, no. 3, pp. 9–13, 1953.

[31] Sugawara, S., Michiyoshi, I., and Minamiyama, T., The Condensation of Vapor Flowing Normal to Horizontal Pipe, *Proc. 6th Jpn. Natl. Congr. Appl. Mech.*, III-4, pp. 385–388, 1956.

[32] Sparrow, E. M. and Gregg, J. L., Laminar Condensation Heat Transfer on a Horizontal Cylinder, *J. Heat Transfer*, vol. 81, pp. 291-296, 1959.
[33] Koh, J. C. Y., Film Condensation in a Forced Convection Boundary-Layer Flow, *Int. J. Heat Mass Transfer*, vol. 5, pp. 941-954, 1962.
[34] Chen, M. M., An Analytical Study of Laminar Film Condensation: Part 2–Single and Multiple Horizontal Tubes, *J. Heat Transfer*, vol. 83, pp. 55-60, 1961.
[35] Berman, L. D. and Tumanov, Y. A., Investigation of Heat Transfer in the Condensation of Moving Steam on a Horizontal Tube, *Teploenergetika*, vol. 9, pp. 77-83, 1962.
[36] Shekriladze, I. G. and Gomelauri, V. I., Theoretical Study of Laminar Film Condensation of Flowing Vapor, *Int. J. Heat Mass Transfer*, vol. 9, pp. 581-591, 1966.
[37] Denny, V. E. and Mills, A. F., Laminar Film Condensation of a Flowing Vapor on a Horizontal Cylinder at Normal Gravity, *J. Heat Transfer*, vol. 91, pp. 495-501, 1969.
[38] Fujii, T., Uehara, H., and Kurata, C., Laminar Filmwise Condensation of Flowing Vapor on a Horizontal Cylinder, *Int. J. Heat Mass Transfer*, vol. 15, pp. 235-246, 1972.
[39] Berman, L. D., Heat Transfer with Condensation of Moving Vapor on a Horizontal Tube, *Teploenergetika*, vol. 20, pp. 76-77, 1973.
[40] Nicol, A. A. and Wallace, D. J., Condensation with Appreciable Vapor Velocity and Variable Wall Temperature, NEL Rept. 619, pp. 27-38, National Engineering Laboratory, East Kilbride, Scotland, August 1976.
[41] Nobbs, D. W., The Effect of Downwaar Vapor Velocity and Inundation on the Condensation Rates on Horizontal Tubes and Tube Banks, Ph.D. thesis, Univ. of Bristol, Bristol, England, April 1975.
[42] Shekriladze, I. G. and Zhorzholiani, G. I., Analysis of the Process of Film Condensation of Moving Vapor on a Horizontal Cylinder, *J. Eng. Phys.*, vol. 25, pp. 818-821, 1975.
[43] Nicol, A. A., Bryce, A., and Ahmed, A. S. A., Condensation of a Horizontally Flowing Vapor on a Horizontal Cylinder Normal to the Vapor Steam, *Heat Transfer 1978*, vol. 2, pp. 401-406, Toronto, 1979.
[44] Fujii, T., Honda, H., and Oda, K., Condensation of Steam on a Horizontal Tube–The Influence of Oncoming Velocity and Thermal Condition of the Tube Wall, in *Condensation Heat Transfer*, eds. P. J. Marto and P. G. Kroeger, pp. 35-43, ASME, New York, 1979.
[45] Kutateladze, S. S., Gogonin, N. I., Dorokhov, A. R., and Sosunov, V. I., Film Condensation of Flowing Vapor on a Bundle of Plain Horizontal Tubes, *Thermal Eng.*, vol. 26, pp. 280-273, 1979.
[46] Gaddis, E. S., Solution of the Two-Phase Boundary-Layer Equations for Laminar Film Condensation of Vapor Flowing Perpendicular to a Horizontal Cylinder, *Int. J. Heat Mass Transfer*, vol. 22, pp. 371-382, 1979.
[47] Berman, L. D., Influence of Vapor Velocity on Heat Transfer with Filmwise Condensation on a Horizontal Tube, *Thermal Eng.*, vol. 26, pp. 274-278, 1979.
[48] Fujii, T., Vapor Shear and Condensate Inundation: An Overview, in *Power Condenser Heat Transfer Technology*, eds. P. J. Marto and R. H. Nunn, pp. 193-223, Hemisphere, New York, 1981.
[49] Honda, H., Nozu, S., and Fujii, T., Vapor to Coolant Heat Transfer during Condensation of Flowing Vapor on a Horizontal Tube, *Heat Transfer 1982*, vol. 5, pp. 77-82, Munich, 1982.
[50] Rosner, D. E., Günes, D., and Anous, N., Aerodynamically Driven Condensate Layer Thickness Distributions on Isothermal Cylindrical Surfaces, *Chem. Eng. Commun.*, vol. 24, pp. 275-287, 1983.
[51] Lee, W. C. and Rose, J. W., Film Condensation on a Horizontal Tube–Effect of Vapor Velocity, *Heat Transfer 1982*, vol. 5, pp. 101-106, Munich, 1982.
[52] Jakob, M., *Heat Transfer*, vol. 1, pp. 667-673, Wiley, New York, 1949.
[53] Short, B. E. and Brown, H. E., Condensation of Vapors on Vertical Banks of Horizontal Tubes, *Proc. Inst. Mech. Eng., London*, General Discussion on Heat Transfer, pp. 27-31, London, 1951.
[54] Fuks, S. N., Heat Transfer with Condensation of Steam Flowing in a Horizontal Tube Bundle, *Teploenergetika*, vol. 4, pp. 35-39, 1957.
[55] Kern, D. Q., Mathematical Development of Loading in Horizontal Condensers, *AIChE J.*, vol. 4, pp. 157-160, 1958.
[56] Watson, R. G. H., Brunt, J. J., and Birt, D. C. P., Dropwise Condensation of Steam, *International Developments in Heat Transfer*, pt. 2, pp. 296-301, ASME, New York, 1961.
[57] Young, E. H. and Briggs, D. E., The Condensing of Low Pressure Steam on Vertical Rows of Horizontal Copper and Titanium Tubes, *AIChE J.*, vol. 12, pp. 31-35, 1966.
[58] Grant, I. D. R. and Osment, B. D. J., The Effect of Condensate Drainage on Condenser Performance, NEL Rept. 350, National Engineering Laboratory, East Kilbride, Scotland, April 1968.
[59] Isachenko, V. P. and Glushkov, A. F., Heat Transfer with Steam Condensing on a Horizontal Tube and with a Flow of Condensate from Above, *Teploenergetika*, vol. 16, pp. 79-81, 1969.
[60] Eissenberg, D. and Bogue, D., Tests of an Enhanced Horizontal Tube Condenser under Conditions of Horizontal Steam Cross Flow, *Heat Transfer 1970*, vol. 1, pp. 1-11, Paris, 1970.
[61] Eissenberg, D. M., An Investigation of the Variables Affecting Steam Condensation on the Outside of a Horizontal Tube Bundle, Ph.D. thesis, Univ. of Tennessee, Knoxville, December 1972.
[62] Fujii, T., Uehara, H., Hirata, K., and Oda, K., Heat Transfer and Flow Resistance in Condensation of Low Pressure Steam Flowing through Tube Banks, *Int. J. Heat Mass Transfer*, vol. 15, pp. 247-260, 1972.
[63] Turek, K., Heat Transfer and Pressure Losses in Film Condensation of Flowing Saturated Steam on Horizontal Nests of Tubes, *Chem. Ing. Tech.*, vol. 44, pp. 280-285, 1972.

[64] Croix, J. M. and Liegeois, A., Condensation in a Horizontal Tube Bundle, Rept. TT/SETRE/78-3-B/JMC, ALi, Centre Nucleaire, Grenoble, France, March 1978.
[65] Shklover, G. G. and Buevich, A. V., The Mechanism of Film Flow with Steam Condensation in Horizontal Bundles of Tubes, *Teploenergetika*, vol. 25, pp. 62–65, 1978.
[66] Butterworth, D., Inundation without Vapor Shear, in *Power Condenser Heat Transfer Technology*, eds. P. J. Marto and R. H. Nunn, pp. 271–277, Hemisphere, New York, 1981.
[67] Berman, L. D., Heat Transfer with Steam Condensation on a Bundle of Horizontal Tubes, *Thermal Eng.*, vol. 28, pp. 218–224, 1981.
[68] Ferguson, R. M. and Oakden, J. C., Heat Transfer Coefficients for Water and Steam in a Surface Condenser, British Electric and Allied Industries Research Association Tech. Rept. H/t 26, London, 1936.
[69] Gudemchuk, V. A., *Teplosilovoe Khoz.*, no. 4, 1980.
[70] Hawes, R. I., Effect of Vapor Cross-Flow Velocity on Condensation, NEL Rept. 619, pp. 55–58, National Engineering Laboratory, East Kilbride, Scotland, August 1976.
[71] Brickell, G. M., Potential Problem Areas in Simulating Condenser Performance, in *Power Condenser Heat Transfer Technology*, eds. P. J. Marto and R. H. Nunn, pp. 51–61, Hemisphere, New York, 1981.
[72] McNaught, J. M., Two-Phase Forced Convection Heat Transfer during Condensation on Horizontal Tube Bundles, *Heat Transfer 1982*, vol. 5, pp. 125–131, Munich, 1982.
[73] Glausser, W. E., Unruh, C. H., and Balekjian, G., Plant Test of a 95,000 Square-Foot Condenser, *Proc. Am. Power Conf.*, vol. 22, pp. 321–331, 1960.
[74] Rowe, M. and Ferrison, J. A., Steam-Side Measurements in the Condenser of a 500 MW Turbine, NEL Rept. 619, pp. 123–129, National Engineering Laboratory, East Kilbride, Scotland, August 1976.
[75] Ferrison, J. A., Rowe, M., and Beckett, G., The Testing of the Ince 'B' Condenser, presented at the EPRI Symposium on State-of-the-Art Condenser Technology, Orlando, Fla., June 1983.
[76] Arnold, G., Changes to ASME PTC 12.2 and TVA Condenser Test Experience, presented at the EPRI Sympoisum on State-of-the-Art Condenser Technology, Orlando, Fla., June 1983.
[77] Clay, C. A. E. and Sochaczewski, Z. W., A New Condenser Test Code and Associated Measurement Techniques, *Condensers: Theory and Practice*, Institution of Chemical Engineers Symp. Ser., no. 75, pp. 171–183, March 1983.
[78] Chisholm, D., Modern Developments in Marine Condensers: Noncondensable Gases: An Overview, in *Power Condenser Heat Transfer Technology*, eds. P. J. Marto and R. H. Nunn, pp. 95–142, Hemisphere, New York, 1981.
[79] Webb, R. L. and Wanniarachchi, A. S., The Effects of Noncondensable Gases in Water Chiller Condenser—Literature Survey and Theoretical Predictions, *ASHRAE Trans.*, vol. 86, pt. 1, pp. 142–159, 1980.
[80] Colburn, A. P. and Hougen, O. A., Design of Cooler Condensers for Mixtures of Vapors with Noncondensing Gases, *Ind. Eng. Chem.*, vol. 26, pp. 1178–1182, 1934.
[81] Bobe, L. S. and Malyshev, D. D., Calculating the Condensation of Steam with a Crossflow of Steam-Gas Mixture over Tubes, *Teploenergetika*, vol. 18, no. 12, pp. 84–86, 1971.
[82] Wanniarachchi, A. S. and Webb, R. L., Noncondensible Gases in Shell-Side Refrigerant Condensers, *ASHRAE Trans.*, vol. 88, pt. 2, 1982.
[83] Berman, L. D. and Fuks, S. N., Mass Transfer in Condensers with Horizontal Tubes when the Steam Contains Air, *Teploenergetika*, vol. 5, no. 8, pp. 66–74, 1958.
[84] Fuks, S. N. and Zernova, E. P., Heat and Mass Transfer with Condensation of Pure Steam and of Steam Containing Air, Supplied from the Side of a Tube Bank, *Teploenergetika*, vol. 17, no. 3, pp. 59–63, 1970.
[85] Sparrow, E. M. and Lin, S. H., Condensation Heat Transfer in the Presence of a Non-Condensable Gas, *J. Heat Transfer*, vol. 86, pp. 430–436, 1964.
[86] Minkowycz, W. J. and Sparrow, E. M., Condensation Heat Transfer in the Presence of Noncondensables, Interfacial Resistance, Superheating, Variable Properties, and Diffusion, *Int. J. Heat Mass Transfer*, vol. 9, pp. 1125–1144, 1966.
[87] Rose, J. W., Approximate Equations for Forced Convection Condensation in the Presence of a Non-Condensing Gas on a Flat Plate and Horizontal Tube, *Int. J. Heat Mass Transfer*, vol. 23, pp. 539–546, 1980.
[88] Rose, J. W., Condensation in the Presence of Noncondensing Gases, in *Power Condenser Heat Transfer Technology*, eds. P. J. Marto and R. H. Nunn, pp. 151–162, Hemisphere, New York, 1981.
[89] Standiford, F. C., Effect of Non-Condensibles on Condenser Design and Heat Transfer, *Chem. Eng. Prog.*, vol. 75, pt. 2, pp. 59–62, 1979.
[90] Meisenburg, S. J., Boarts, R. M., and Badger, W. L., *Trans. AIChE*, vol. 31, pp. 622–638, 1935; vol. 32, pp. 100–104 and 449–450, 1936.
[91] Coit, R. L., A Designer's Approach to Surface Condenser Venting and Deaeration, in *Power Condenser Heat Transfer Technology*, eds. P. J. Marto and R. H. Nunn, pp. 163–180, Hemisphere, New York, 1981.
[92] Rowe, M., Condenser Improvements, *UK/USSR Symposium 1976*, Rept. 4, pp. 1–5, Central Electricity Research Laboratories, Leatherhead, U.K., May 1976.
[93] Bergles, A. E., Enhancement of Heat Transfer, *Proc. 6th Int. Heat Transfer Conf.*, vol. 6, pp. 89–108, Toronto, 1978.
[94] Bergles, A. E., Bibliography on Augmentation of Convective Heat and Mass Transfer, *Previews Heat Mass Transfer*, vol. 4, no. 4, July 1978.
[95] Junkhan, G. H., Bergles, A. E., and Webb, R. L.,

Research Workshop on Energy Conservation through Enhanced Heat Transfer, HTL-21, Iowa State Univ., Ames, Iowa, May 1979.
[96] Nakayama, W., Enhancement of Heat Transfer, *Heat Transfer 1982*, vol. 1, pp. 223–240, Hemisphere, New York, 1982.
[97] Webb, R. L., The Use of Enhanced Surface Geometries in Condensers: An Overview, in *Power Condenser Heat Transfer Technology*, eds. P. J. Marto and R. H. Nunn, pp. 287–324, Hemisphere, New York, 1981.
[98] Cooper, J. R. and Rose, J. W., Condensation Heat Transfer Enhancement by Vapor-Side Surface Geometry Modification, HTFS Research Symposium, pp. 647–672, HTFS Harwell and National Engineering Laboratory, U. K., 1981.
[99] Marto, P. J. and Nunn, R. H., A Critical Review of Heat Transfer Enhancement Techniques for Use in Marine Condensers, NPS 69-82-006, Naval Postgraduate School, Monterey, Calif., 1982.
[100] Gogonin, I. I. and Dorokhov, A. R., Enhancement of Heat Transfer in Horizontal Shell-and-Tube Condensers, *Heat Transfer–Sov. Res.*, vol. 13, no. 3, pp. 119–126, 1981.
[101] Tanasawa, I., Dropwise Condensation: The Way to Practical Applications, *Proc. 6th Int. Heat Transfer Conf.*, vol. 6, pp. 393–405, Toronto, 1978.
[102] Brown, A. R. and Thomas, M. A., Filmwise and Dropwise Condensation of Steam at Low Pressure, *Proc. 3d Int. Heat Transfer Conf.*, vol. 2, pp. 300–305, Chicago, 1966.
[103] Spalvins, T., Coatings for Wear and Lubrication. *Thin Solid Films*, vol. 53, pp. 285–300, 1978.
[104] Beatty, K. D. and Katz, D. L., Condensation of Vapors on Outside of Finned Tubes, *Chem. Eng. Prog.*, vol. 44, pp. 55–70, 1948.
[105] Staub, F. W., Heat Transfer for Film Condensation on Vertical and Horizontal Fluted Tubes, General Electric Rept. 61GL175, Schenectady, N.Y., 1961.
[106] Karkhu, V. A. and Borovkov, V. P., Film Condensation of Vapor at Finely Finned Horizontal Tubes, *Heat Transfer–Sov. Res.*, vol. 3, pp. 183–191, 1971.
[107] Carnavos, T. C., An Experimental Study: Condensing R-11 on Augmented Tubes, ASME paper 80-HT-54, 19th National Heat Transfer Conf., Orlando, Fla., July 1980.
[108] Kisaragi, T., Enya, S., Ochiai, J, Jr., Kuwahara, K., and Tanasawa, I., On the Augmentation of Condensation Heat Transfer on Horizontal Pipes, preprint, Japanese Society of Mechanical Engineering, No. 780-1, p. 1, 1978 (in Japanese).
[109] Arai, N., Fukushima, T., Arai, A., Nakajima, T., Fujii, K., and Nakayama, Y., Heat Transfer Tubes Enhancing Boiling and Condensation in Heat Exchangers of a Refrigerating Machine, *ASHRAE Trans.*, vol. 83, pt. 2, 1977.
[110] Gregorig, R., Film Condensation on Finely Rippled Surfaces with Consideration of Surface Tension, *Z. Angew. Math. Phys.*, vol. 5, pp. 36–49, 1954 (transl. D. K. Edwards).
[111] Edwards, D. K., Gier, K. D., Ayyaswamy, P. S., and Catton, I., Evaporation and Condensation in Circumferential Grooves on Horizontal Tubes, ASME paper 73-HT-25, 12th National Heat Transfer Conf., Atlanta, Ga., August 1973.
[112] Mori, Y., Hijikata, K., Hirasawa, S., and Nakayma, W., Optimized Performance of Condensers with Outside Condensing Surface, in *Condensation Heat Transfer*, eds. P. J. Marto and P. G. Kroeger, pp. 55–62, ASME, New York, 1979.
[113] Shklover, G. G., Milman, O. O., Baskov, V. S., and Aukudinov, G. A., Heat Transfer in Condensation of Steam on Finely Finned Horizontal Tubes, *Heat Transfer–Sov. Res.*, vol. 13, no. 2, pp. 108–114, March-April 1981.
[114] Thomas, G. G., Condenser Tube, U.S. patent 3,358,750, December 19, 1967.
[115] Thomas, A., Lorenz, J. J., Hillis, D. L., Yung, D. T., and Sather, N. F., Performance Tests of the 1 MW_t Shell-and-Tube Heat Exchangers for OTEC, presented at the 6th OTEC Conf., Washington, D.C., June 1979.
[116] Withers, J. G. and Young, E. H., Steam Condensing on Vertical Rows of Horizontal Corrugated and Plain Tubes, *Ind. Eng. Chem. Process Des. Dev.*, vol. 10, pp. 19–20, January 1971.
[117] Palen, J., Cham, B., and Taborek, J., Comparison of Condensation of Steam on Plain and Turbotec Spirally Grooved Tubes in a Baffled Shell-and-Tube Condenser, Rept. 2439-300/6, Heat Transfer Research, Inc., Alhambra, Calif., January 1971.
[118] Young, E. H., Withers, J. G., and Lampert, W. B., Heat Transfer Characteristics of Corrugated Tubes in Steam Condensing Applications, AIChE paper 3, 15th National Heat Transfer Conf., San Francisco, Calif., August 1975.
[119] Catchpole, J. P. and Drew, B. C. H., Evaluation of Some Shaped Tubes for Steam Condensers, in *Steam Turbine Condensers*, NEL Rept. 619, National Engineering Laboratory, East Kilbride, Glasgow, U.K., August 1976.
[120] Mehta, M. H. and Rao, M. R., Heat Transfer and Frictional Characteristics of Spirally Enhanced Tubes for Horizontal Condensers, *Advances in Enhanced Heat Transfer*, pp. 11–22, ASME, New York, August 1979.
[121] Glicksman, L. R., Mikic, B. B., and Snow, D. F., Augmentation of Film Condensation on the Outside of Horizontal Tubes, *AIChE J.*, vol. 19, no. 3, pp. 636–637, May 1973.
[122] Desmond, R. M. and Karlekar, B. V., Experimental Observations of a Modified Condenser Tube Design to Enhance Heat Transfer in a Steam Condenser, ASME paper 80-HT-53, 19th National Heat Transfer Conf., Orlando, Fla., July 1980.
[123] Rudy, T. M. and Webb, R. L., Condensate Retention of Horizontal Integral-Fin Tubing, *Advances in Enhanced Heat Transfer–1981*, pp. 35–42, ASME, New York, August 1981.
[124] Private communication, Linde Division, Union Carbide Corp., Tonawanda, N.Y., July 29, 1982.
[125] *Heat Exchanger Design Handbook*, vol. 2, chap. 2.2.4, Hemisphere, New York, 1982.
[126] Knudsen, J. G. and Katz, D. L., *Fluid Dynamics*

and Heat Transfer, p. 338, McGraw-Hill, New York, 1958.

[127] Eissenberg, D. M., Personal communication, Oak Ridge National Laboratory, Oak Ridge, Tenn., September 28, 1977.

[128] Mueller, A. C., Pressure Drop, *Heat Exchanger Design Handbook*, vol. 3, p. 3.4.7-1, Hemisphere, New York, 1982.

[129] Lee, N. K., Hollingsworth, M. A., and Mayhew, Y. R., Simulation of Condenser Pressure Losses by Porous Tubes with Suction, *Heat Transfer 1982*, vol. 5, pp. 107–112, Munich, 1982.

[130] Aly, S. and Cunningham, J., Effect of Mass Transfer on Flow across a Staggered Tube Bundle, *Int. J. Heat Fluid Flow*, vol. 1, no. 4, pp. 169–175, 1979.

[131] Nicol, A. A., Aidoun, Z., and Musa, M. N., Condensation and Pressure Drop for Crossflow of Steam in Small Tube Bundles, *Heat Transfer 1982*, vol. 5, pp. 133–138, Munich, 1982.

[132] Diehl, J. E., Calculate Condenser Pressure Drop, *Pet. Refiner*, vol. 36, no. 10, pp. 147–153, 1957.

[133] Collier, J. G., *Convective Boiling and Condensation*, pp. 341–343, McGraw-Hill, New York, 1972.

[134] Diehl, J. E. and Unruh, C. H., Two Phase Pressure Drop for Horizontal Crossflow through Tube Banks, *Petroleum Refiner*, vol. 37, no. 10, pp. 124–128, 1958.

[135] Wallis, G. B., *One Dimensional Two-Phase Flow*, McGraw-Hill, New York, 1969.

[136] Grant, I. D. R. and Chisholm, D., Two-Phase Flow on the Shell-Side of a Segmentally Baffled Shell-and-Tube Heat Exchanger, *J. Heat Transfer*, vol. 101, pp. 38–42, 1979.

[137] Grant, I. D. R., Chisholm, D., and Cotchin, C. D., Shellside Flow in Horizontal Condensers, ASME paper 80-HT-56, ASME/AIChE 19th National Heat Transfer Conference, Orlando, Fla., July 1980.

[138] Grant, I. D. R. and Chisholm, D., Horizontal Two-Phase Flow across Tube Banks, *Int. J. Heat Fluid Flow*, vol. 2, no. 2, pp. 97–100, 1980.

[139] Grant, I. D. R. and Murray, I., Pressure Drop on the Shell-Side of Segmentally Baffled Shell-and-Tube Heat Exchanger with Horizontal Two-Phase Flow, NEL Rept. 560, National Engineering Laboratory, East Kilbride, Scotland, 1974.

[140] Baker, O., Simultaneous Flow of Oil and Gas, *Oil Gas J.*, vol. 53, no. 12, pp. 185–190, 1954.

[141] Bell, K. J., Taborek, J., and Fenoglio, F., Interpretation of Horizontal In-Tube Condensation Heat Transfer Correlations with a Two-Phase Flow Regime Map, *Chem. Eng. Prog. Symp. Ser.*, vol. 66, no. 102, pp. 150–165, 1970.

[142] Breber, G., Palen, J. W., and Taborek, J., Prediction of Horizontal Tubeside Condensation of Pure Components using Flow Regime Criteria, *Condensation Heat Transfer*, pp. 1–8, ASME, New York, 1979.

[143] Tandon, T. N., Varma, H. K., and Gupta, C. P., A New Flow Regimes Map for Condensation inside Horizontal Tubes, *J. Heat Transfer*, vol. 104, pp. 763–768, 1982.

[144] Ishihara, K., Palen, J. W., and Taborek, J., Critical Review of Correlations for Predicting Two-Phase Flow Pressure Drop across Tube Banks, *Heat Transfer Eng.*, vol. 1, no. 3, pp. 23–32, 1980.

[145] Kistler, R. S. and Kassem, A. E., Stepwise Rating of Condensers, *Chem. Eng. Prog.*, vol. 77, no. 7, pp. 55–59, 1981.

[146] Sha, W. T., Yang, C. I., Kao, T. T., and Cho, S. M., Multidimensional Numerical Modeling of Heat Exchangers, *J. Heat Transfer*, vol. 104, pp. 417–425, 1982.

[147] Shklover, G. G. and Grigorev, V. G., Calculating the Heat Transfer Coefficient in Steam Turbine Condensers, *Teploenergetika*, vol. 22, no. 1, pp. 67–71, 1975.

[148] Barsness, E. J., Calculation of the Performance of Surface Condensers by Digital Computer, ASME paper 63-PWR-2, National Power Conf., Cincinnati, Ohio, September 1963.

[149] Hafford, J. A., ORCON1: A Fortran Code for the Calculation of a Steam Condenser of Circular Cross Section, ORNL-TM-4248, Oak Ridge National Laboratory, Oak Ridge, Tenn., July 1973.

[150] Emerson, W. H., The Application of a Digital Computer to the Design of Surface Condensers, *The Chemical Engineer (London)*, No. 228, pp. 178–184, May 1969.

[151] Wilson, J. L., *The Design of Condensers by Digital Computers*, Institution of Chemical Engineers Symp. Ser., no. 35, pp. 21–27, 1972.

[152] Davidson, B. J., Flow of Steam in a Tube Nest—Numerical Analysis, in *UK/USSR Symposium 1976*, Rept. 5, sect. 5.2, Central Electricity Research Laboratories, Leatherhead, U.K., May 1976.

[153] Butterworth, D., Modeling of the Gas/Vapor Phase Flow, in *Power Condenser Heat Transfer Technology*, eds. P. J. Marto and R. H. Nunn, pp. 75–81, Hemisphere, New York, 1981.

[154] Shida, H., Kuragasaki, M., and Adachi, T., On the Numerical Analysis Method of Flow and Heat Transfer in Condensers, *Heat Transfer 1982*, vol. 6, pp. 347–352, Munich, 1982.

[155] Ukeguchi, N., Sakata, H., and Adachi, T., On the Numerical Analysis of Compressible Flow Problems by the Modified FLIC Method, *Comput. Fluids*, vol. 8, pp. 251–263, 1980.

[156] Marto, P. J. and Nunn, R. H., The Potential of Heat Transfer Enhancement in Surface Condensers, *Condensers: Theory and Practice*, Institution of Chemical Engineers Symp. Ser., no. 75, pp. 171–183, March 1983.

[157] Johnson, C. M., Vanderplaats, G. N., and Marto, P. J., Marine Condenser Design using Numerical Optimization, *J. Mech. Des.*, vol. 102, pp. 469–475, 1980.

[158] Mayhew, Y. R., Additional Observations on Vapor Shear and Condensate Inundation, in *Power Condenser Heat Transfer Technology*, eds. P. J. Marto and R. H. Nunn, pp. 229–230, Hemisphere, New York, 1981.

P. J. Marto is a professor of mechanical engineering at the Naval Postgraduate School. He received a B.S. degree from the University of Notre Dame and S.M. and Sc.D. degrees from the Massachusetts Institute of Technology. He has been teaching at the Naval Postgraduate School since 1965, except for one year which he spent at the U.S. Naval Academy. In 1978 he was appointed chairman of the Department of Mechanical Engineering. His research contributions include basic works on nucleate boiling, condensation, and enhanced heat transfer, as well as applied works on stationary and rotating heat pipes. He is co-editor of the book *Power Condenser Heat Transfer Technology* (Hemisphere, 1981). Active in the Heat Transfer Division of ASME, he is currently chairman of the Committee on Honors and Awards and a technical editor of the *Journal of Heat Transfer*.